Front. Chem. Sci. Eng. 2025, 19(12): 119
https://doi.org/10.1007/s11705-026-2627-9

REVIEW ARTICLE

Electrodeposited high-entropy alloys as electrocatalysts in water electrolysis for hydrogen production: a review on impacts of composition and synthesis parameters

Daniela Arango (✉), Antonio G. De Crisci (✉), Rafal Gieleciak, Mathieu L'Abbe, Jinwen Chen

Natural Resources Canada, CanmetENERGY, Devon AB, T9G 1A8, Canada

Abstract High-entropy alloys are described as materials that have equiatomic and multi-element compositions. Their unique atomic structure may provide alternative electrocatalysts for water electrolysis over traditional and expensive noble metal-based catalysts, delivering superior catalytic activity and stability. Among various high-entropy alloys synthesis methods, electrodeposition stands out as a versatile and cost-effective approach due to its mild conditions and precise control over composition and deposition properties. This review focuses on noble metal-free high-entropy alloys prepared by electrodeposition, with applications in water electrolysis. The impacts of alloying elements and electrodeposition parameters on the morphology, composition, and electrochemical performance of the resulting coatings for hydrogen evolution reaction and oxygen evolution reaction are also examined. The roles of key alloying elements are discussed, including their individual contributions during the electrodeposition process, interactions within the bath, and effects on the final coating. The review also discusses critical deposition parameters such as bath chemistry, pH value, current density, temperature, and bath agitation, and their influences on properties and electrochemical activity of electrodeposited coatings. Finally, future research directions and recommendations in several key areas are outlined to address important knowledge gaps for further advancing the optimization and application of electrodeposited high-entropy alloys as effective electrocatalysts for water electrolysis.

Keywords hydrogen, high-entropy alloys (HEAs), electrodeposition (ED), water electrolysis, electrocatalysts

Received July 29, 2025; accepted September 24, 2025;
online December 1, 2025

E-mails: daniela.arangovasquez@nrcan-rncan.gc.ca (Arango D.),
antonio.decrisci@nrcan-rncan.gc.ca (De Crisci A. G.)

1 Introduction

High-entropy alloys (HEAs) are an emerging class of advanced materials made of multiple principal elements in near-equiatomic ratios to create unique chemical and structural properties [1]. This distinctive composition enhances their electrocatalytic activity, making HEAs promising candidates for hydrogen production via water electrolysis.

When powered by renewable electricity, H_2 produced by water electrolysis is classified as green hydrogen, which has a significantly lower carbon footprint compared to conventional methods such as steam methane reforming and coal gasification [2]. Despite extensive research and development over the years, large-scale implementation of water electrolysis technologies has been hindered by persistent scientific and technological challenges, including inefficiencies in reaction kinetics, overall durability, as well as economic barriers stemming from the utilization of specialized infrastructure and the dependence on precious metal catalysts [3,4].

Emerging research aims to develop efficient catalysts to lower overpotential, reduce energy consumption, and increase the overall efficiency of hydrogen production via water electrolysis [5]. To understand how catalysts can improve efficiency, it helps to examine the individual components that make up the total cell potential, as shown in Eq. (1) [6].

$$E_{\text{cell}} = E^0_{\text{cell}}(p,T) + \eta_{\text{kin}} + \eta_{iR} + \eta_{\text{mtx}}, \quad (1)$$

where $E^0_{\text{cell}}(p,T)$ is the reversible cell potential, which represents the thermodynamic minimum voltage required to split water (1.23 V at 25 °C, 1.013×10^5 Pa). η_{kin} is the kinetic overpotential, or activation overpotential, which represents the extra energy required to overcome the kinetic barriers of the oxygen evolution reaction (OER) and hydrogen evolution reaction (HER) at the anode and

cathode, respectively (Fig. 1(a)). This overpotential is influenced by the intrinsic activity of the catalyst (often determined by its composition), the specific reaction pathway, and the active electrochemical surface area (ECSA). Enhancing the catalyst's activity reduces η_{kin} allowing the same current density to be reached at a lower applied voltage [7]. The η_{iR} term represents ohmic losses, which arise from the resistance to electron flow through the cell components, and ion transport through the electrolyte and membrane [8]. From the catalyst side, ohmic losses can be reduced by using materials with high conductivity, optimized thickness, strong catalyst/substrate adhesion, and low contact resistance [9]. Finally, η_{mtx} is the mass transport overpotential, which occurs when reactants cannot reach the electrode fast enough or products cannot leave quickly enough. The catalyst's architecture strongly influences this term; porous structures enhance ion and molecule transport and promote rapid bubble detachment, preventing active site blockage and providing multiple pathways for efficient reactant and product flow [10].

As shown in Fig. 1(b), all overpotential components such as η_{kin}, η_{iR}, and η_{mtx} tend to increase with current density. As a result, the system experiences larger energy losses, meaning higher applied voltages are needed to maintain the desired reaction rate. These trends show the potential benefits of optimizing catalysts, particularly in lowering energy losses and allowing efficient operation at high current densities. It is important to note that besides catalysts, overpotential can also be reduced through cell design, operating conditions (temperature, pressure, and flow), and membrane selection, all of which strongly influence efficiency.

Pt and Ir based catalysts are widely considered to be the most effective ones for water electrolysis. However, due to their high cost, research on developing lower-cost electrocatalysts based on more abundant materials has been actively conducted [12]. Non-noble metal electrocatalysts are highly desired due to their low cost and high availability. However, their reactivity toward electrocatalytic water splitting reaction to produce hydrogen is usually lower than that of noble metals-based ones, resulting in reduced performance, stability, and/or selectivity. One approach to addressing these performance limitations is to alloy single-metal catalysts with one or more additional metal elements [13]. Electrocatalysts, with multiple metals such as nickel-iron and nickel-iron-cobalt alloys (NiFe, NiFeCo), have been the subject of extensive research [14,15]. They are considered traditional alloys and are synthesized by blending one or two principal elements with minor additives [16]. Over the years, research has focused on exploring new compositions for improved efficiency, reduced production cost, enhanced stability, and minimized environmental footprint [17,18]. A revolutionary alloying method emerged in the early 2000s, which involved combining multiple elements in nearly equal proportions to maximize the configurational entropy of mixing (ΔS_{mix}), which is defined by Eq. (2). This high entropy is believed to stabilize single-phase solid solutions, resulting in the formation of HEAs [12,19,20]. As shown in Eq. (2), ΔS_{mix} is related to the number of elements (n) and their molar fractions (x_i), whereas R is the gas constant. A greater number of elements with similar atomic fractions increases the mixing entropy, promoting the formation of multi-element solid solutions. Alloys can be classified as high-, medium-, or low-entropy alloys (HEAs, MEAs, or LEAs) based on their configurational entropy. HEAs typically have ΔS_{mix} higher than 1.5R, whereas LEAs normally have ΔS_{mix} below 1R and MEAs are in between HEAs and MEAs [21]. Most conventional alloys are considered LEAs.

$$\Delta S_{mix} = -R\sum_{i=1}^{n} x_i \ln(x_i). \quad (2)$$

The term 'HEA' was first introduced by Yeh in the US patent application US2002159914-A1 in 2002 [22]. Since then, HEAs have attracted increasing attention from the R&D community because of their unique structures and outstanding properties. The four commonly referred core effects of HEAs include: (1) high entropy (single phase stability), (2) lattice distortion (defect-driven properties improvement), (3) sluggish diffusion (reduced atomic mobility; higher stability), and (4) cocktail effects (synergistic properties among elements) [20].

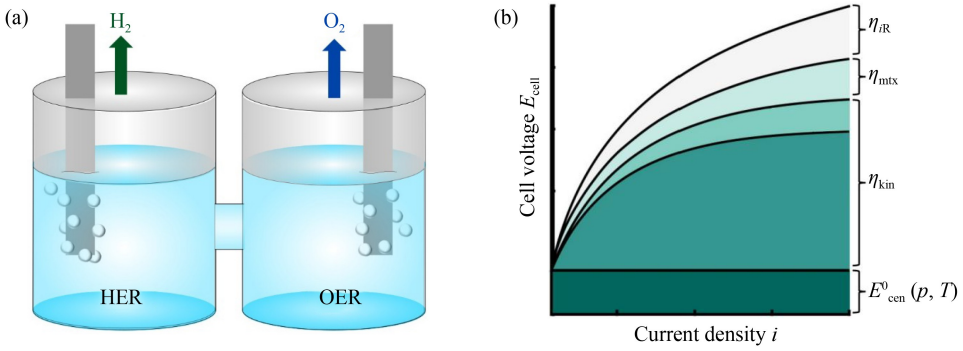

Fig. 1 (a) Schematic illustration of an electrochemical water-splitting cell. (b) Schematic diagram of the cell voltage breakdown and current dependence. Reprinted with permission from Ref. [11], copyright 2020, Electrochemical Society.

Early research on HEAs focused on their complex atomic arrangements and physical properties, such as their exceptional mechanical properties [23,24], and high corrosion resistance [25], which have led to their promising potential for various industrial applications [26]. The following research illuminated the idea of using them as catalysts for common electrochemical reactions [27], such as HER [28,29], OER [30,31], methanol oxidation [32], and CO_2 conversion [33,34]. HEAs have since demonstrated great potential in electrocatalysis, offering precisely tunable electronic and morphological structures, rapid reaction kinetics, and remarkable stability under strong acidic or basic conditions [19,35]. All these advantages are driven by their core effects and ability to provide a diverse array of active catalytic sites for multiple reactions [36].

Built on the success in electrocatalysis, HEAs have demonstrated great potential toward electrolysis of water to produce hydrogen. One of the early studies demonstrating noble metal-free HEAs for water electrolysis was published by Zhang et al. [37] in 2018 to show the efficacy of a CoCrFeNiMo HEA for HER in acidic and alkaline electrolytes. The study highlighted the HEA intrinsic properties, such as high entropy of mixing for stable solid solution formation and its unique composition, which provided improved corrosion resistance and catalytic efficiency [37]. Subsequent studies explored various HEA compositions and advanced the transition from bulk materials to nanostructured morphologies with enhanced surface area. These efforts also provided deeper insight into the high capabilities of HEAs in water-splitting applications. Figure 2 illustrates some key advantages of HEAs for water electrolysis. For HER, HEAs have been demonstrated to have the ability to reduce energy barriers for water dissociation and hydrogen adsorption/desorption, which can be further enhanced by electronegativity differences among the different components that create modulation of the adsorption energy distribution [38,39]. Under alkaline conditions, HEAs typically retain their metallic surface during HER, preserving their activity. In contrast, during OER the surface often transforms into layered double hydroxides which are real active centers of OER electrocatalysts [40], and together with their unique electronic properties and induced strain from lattice distortion can provide fast electron-transport speeds, abundant active sites, and enhanced oxygen desorption, leading to superior OER catalytic performance [41−43]. Regarding chemical stability, some HEAs are highly resistant to corrosion due to their homogeneous phase structure, which prevents the formation of weak spots where localized corrosion typically occurs [44]. The electronegativity difference between neighboring elements is also believed to help stabilize the material by minimizing electron loss. Additionally, HEAs can be formulated to promote the formation of protective passive films that further enhance their stability and longevity during operation [20,45,46]. While oxidation during OER has been well established and expected [47,48], growing evidence has shown that self-reconstructed oxide layers could also form during alkaline HER, and they could enhance catalytic performance [49]. The addition of elements such as P, B, and O can form high-entropy (HE) phosphides, borides, oxides, and other common compounds such as nitrides, carbides, fluorides, and selenides [50].

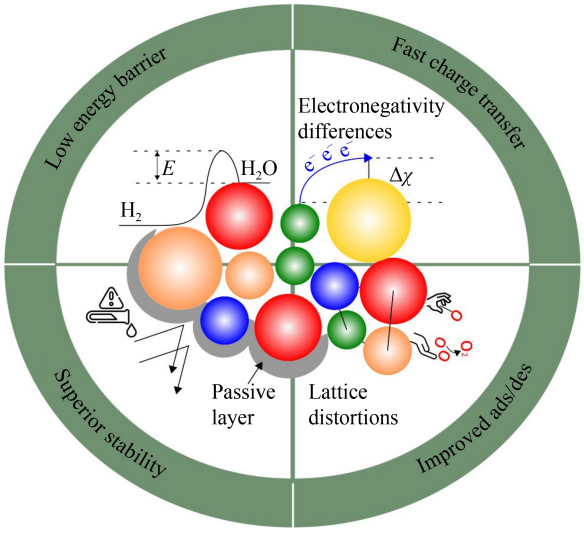

Fig. 2 Schematic representation of the beneficial properties of HEAs enhancing their electrocatalytic activity in water electrolysis.

Figure 3 presents the electrochemical performance of various catalysts for HER under alkaline conditions reported in the literature, as indicated by their Tafel slopes and overpotential values (Table S1, cf. Electronic Supplementary Material, ESM). The data points, represented by different colors, correspond to distinct entropy classifications of noble metal-free materials (e.g., low-entropy (LE), medium-entropy (ME), and HE). The shaded ellipses define the regions associated with entropy categories, including noble metal-containing HE materials (NM HE) and traditional noble metal catalysts (NM CA). Electrocatalysts which require low electrical energy input but exhibit high reaction activity for water splitting, have lower overpotential and Tafel slope values.

The abundance and distribution of data in Fig. 3 reflects the extensive research conducted on LE catalysts, which occupy a broader region in the plot. In contrast, available data for HE and ME materials is limited, reflecting the relatively recent and still-emerging interest in their electrocatalytic properties. NM CA and NM HEA catalysts occupy narrower regions in the plot. Among these, NM HEAs shows a more concentrated distribution near the high-performance region, suggesting that multi-component systems offer enhanced catalytic activity. HE catalysts concentrate in the bottom-left region, exhibiting low energy activation (low overpotential) and rapid

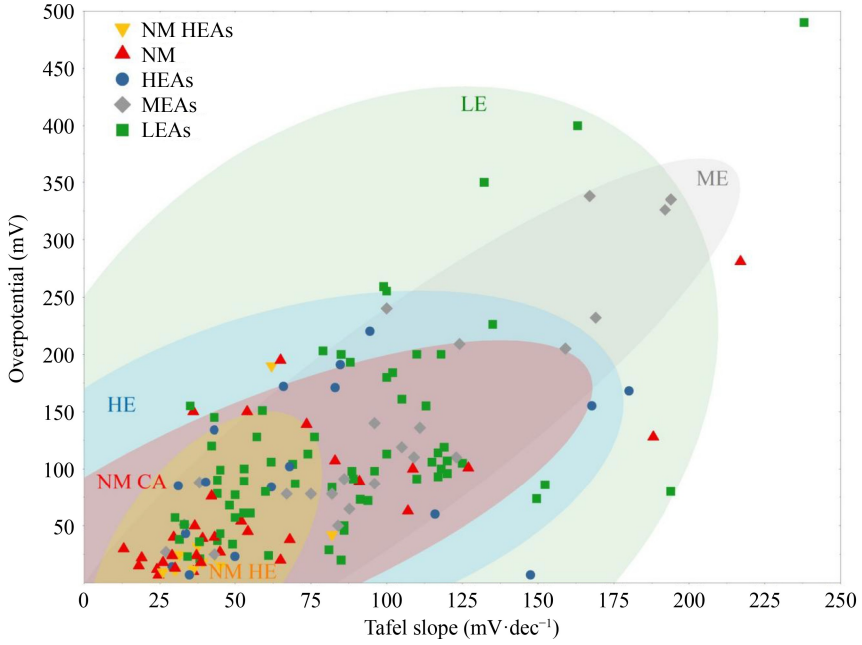

Fig. 3 Alkaline HER performance (overpotential and Tafel slopes) of electrocatalysts from the literature and 90% confidence ellipses (reported activity in 1 mol·L^{-1} KOH at an overpotential of 10 mA·cm^{-2} was compiled from literature sources (see Table S1, cf. ESM)). N.B. Although cathodic Tafel slopes are mathematically negative, all HER-based Tafel slope values summarized here are shown as positive (mV·dec^{-1}), as they were reported in the original publications and follow common convention in the field.

reaction kinetics (low Tafel slope). While NM HEA delivers higher overall performance, the significant overlap between HE and NM CA in the bottom-left region demonstrates the potential of HE catalysts to achieve comparable HER catalytic efficiency.

Other parameters of interest to assess electrochemical activity include exchange current density (j_0) and electrical conductivity. j_0 is a kinetic performance parameter that measures the intrinsic electrocatalytic activity of an electrocatalyst [51,52]. It is calculated using Tafel plots at equilibrium, and high values indicate high electrocatalytic efficiency. Nobel metal-based systems containing Pt, Ir, and Rh are known to have high j_0 [53], however, their cost and availability may outweigh their performance. Some HEAs have shown to have j_0 values comparable to or even exceeding those of noble metal-based catalysts. For example, PtFeCoNiCu HEA exhibited higher j_0 than the conventional Pt/C [54]. In another study, the high j_0 on HEAs was attributed to the optimized binding energy between the catalyst surface and intermediates during HER and OER, arising from the strain induced by the multiatomic composition [55].

Electrical conductivity of HEAs is largely unexplored but is considered a critical parameter that influences performance of these materials as electrocatalysts have to facilitate the efficient transfer of electrons. HEAs typically have lower conductivity than pure metals and metal-based materials (e.g., Cu, Al, and metal oxides) due to their lattice distortions, and atomic disorder. Their electrical conductivity is attributed to the cocktail effect in which the final conductivity differs from that one of constituent elements [56]. More studies on conductivity of HEAs are required.

The application of HEAs in large-scale hydrogen production from water electrolysis necessitates an industrial-compatible manufacturing process to reduce cost, complexity, and energy demand. Some of the electrochemical performance metrics reported in the literature for HEAs correspond to bulk materials characterized by limited surface area, irregular morphology, and large particle size distribution. These alloys are typically synthesized at high temperatures, which requires significant energy input and thus may limit their large-scale production [57,58]. Traditional synthesis methods, such as arc casting and induction furnace smelting, restrict the inclusion of high melting point elements like W (3422 °C) into the alloy. Some advanced methods, such as magnetron sputtering and laser cladding, require specialized and complex equipment [59]. To address these limitations and explore synthesis methods that use milder conditions, electrodeposition (ED) has emerged as an efficient and rapid synthesis method for producing HEA coatings with increased surface area and activity. This technique, with relatively low cost and non-intensive use of equipment, requires only mild conditions, allowing for easy tuning of deposition parameters and microstructure [60,61]. It offers scalability, simplicity, uses readily available infrastructure, and is mostly operated in an aqueous solution at ambient or near-ambient temperatures [29,62]. It also has fewer limitations compared to other larger-scale catalyst production techniques, as it is primarily

constrained by the size of ED bath, and the current capacity of the power source [63].

In general, ED has been used for over a century to produce metal coatings from ionic solutions [64]. For example, ED of Cr, Zn, Cu, and Au is well-established and widely used in industry. However, simultaneously depositing multiple metal elements to create HEAs is challenging. Despite the rising interest in ED to create HEAs, its industrial adoption remains in its early stages due to the complexity of the electrolyte bath, which involves multiple metallic precursors and different reduction potentials. Challenges such as the lack of comparable studies and inconsistent ED conditions make it difficult to use ED for making HEAs toward wider applications. In addition, the variations in compositions of HEAs are extensive, among which only a small portion has been investigated. Some researchers have contributed to the understanding of the fabrication of HEA through ED by reviewing key processing parameters and their effects on the final coatings. This included the effect of direct and pulsed ED techniques on the coating's microstructure, as well as on corrosion resistance and magnetic properties, in addition to a review into their structural and functional potential applications [62,65]. Moreover, a separate study summarized earlier literature on critical deposition parameters, discussing their role in determining coating quality and overall performance [66]. While these reviews offer valuable insights into the fabrication and general properties of electrodeposited HEAs (ED-HEAs), a clear gap remains in optimizing ED-HEA coating specifically for water electrolysis applications as most studies have focused on structural or protective properties rather than on electrocatalysis.

This review summarizes published studies on ED-HEAs toward catalytic water electrolysis and discusses the associated challenges by identifying the role and behavior of different components in the prepared HEA coatings. The influences of ED parameters, such as current density, bath composition, electrolyte pH, ED time, and stirring rate, on the composition, morphology, and electrocatalytic performance of HEA coatings are discussed.

2 ED for making HEA coatings

2.1 The ED technique

ED involves the reduction of metal ions (M^{n+}) onto a conductive substrate, as shown in Eq. (3). The process is primarily governed by each element's ability to accept electrons, which is indicated by its standard reduction potential ($E°$). A more positive $E°$ means an element is more easily reduced. This property is key for co-depositing multiple metals. For example, Cu has a higher $E°$ and is often preferentially deposited over elements with lower $E°$ values.

$$M^{n+} + ne^- \rightarrow M(\text{cathodic reaction}) \quad (3)$$

The basic ED setup consists of an anode, cathode (substrate), electrolyte (metal salt solution), and a power supply [62]. When an electric current is applied, a thin metal layer forms on the cathode as shown in Fig. 4. This process is influenced by three main factors: the ease of electron transfer (charge transfer), the movement of ions through the solution (mass transport), and the applied current. At low current, metal deposition is controlled by charge transfer, but at higher current, ion consumption at the surface can exceed replenishment from the bulk, making the process diffusion-limited and controlled by ion transport instead of surface reactions.

In addition to these core properties, ED is also influenced by external factors such as temperature, stirring, time, and bath composition. The complexity of the process increases when multiple elements are involved as their interactions introduce additional challenges. These factors must be carefully examined and controlled to achieve high-quality coating.

2.2 Studies on electrodeposited HEAs

Pioneering studies by Yao et al. [67] demonstrated the success of ED for the preparation of a BiCoNiMn HEA film on Cu using an organic bath, resulting in advanced coatings with promising potential for magnetic and photo-electronic applications. This foundational work revealed the potential of ED for developing functional HEA coatings and opened the door for further research. Following this study, various HEA compositions and ED methods were investigated, and the use of aqueous baths became more popular with early studies primarily focusing on ED-HEAs for corrosion protection coatings.

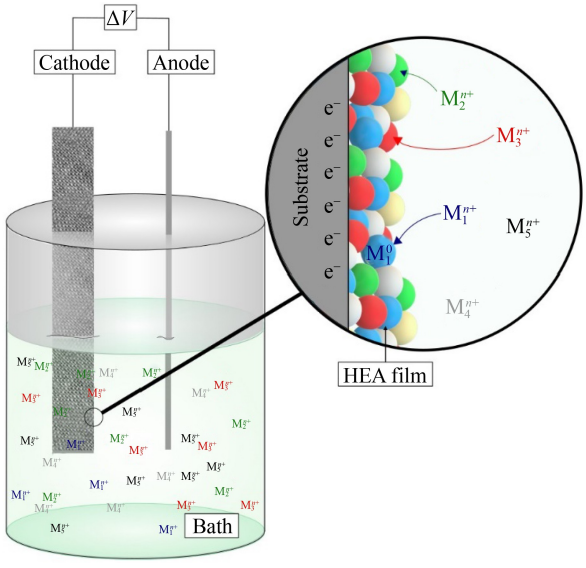

Fig. 4 Schematic illustration of the ED of HEA coatings.

These studies highlighted the excellent corrosion resistance of HEA coatings due to their locally disordered chemical environment, which promotes the formation of a more complex and protective corrosion layer [44,68]. In recent years, research on HEA coatings has expanded to their electrocatalytic applications in processes such as CO_2 conversion, oxygen reduction reaction, water splitting, and glycerol valorization [20,55,69−73]. One of the most advanced outcomes from recent studies on ED-HEAs is the achievement of ultra-low overpotentials for HER with some alloys, such as the electrodeposited NiFeCoMnV, demonstrating an overpotential (η_{10}) as low as 7 mV [74]. Such ultra-low overpotential makes HEAs a promising option for next-generation electrocatalysts, surpassing the performance of conventional noble-metal based catalysts.

The ED methods, operating parameters, and alloy compositions vary significantly among different studies as discussed in detail in the following sections. Table S2 (cf. ESM) summarizes published literature on ED-HEAs with potential application in water electrolysis. The table provides detailed information on their composition and ED parameters, including substrate material, electrolytic bath, ED current, pH value, temperature, deposition time, and stirring speed. Additionally, it includes their final morphology, thickness, and HER and/or OER activities, where available.

2.3 Composition of electrodeposited HEAs for water electrolysis

Compared to single-metal catalysts, which often have low performance and stability to limit their applications, HEAs with abundant transition metals such as Ni, Fe, Cr, Co, Mn, and Cu, exhibit high stability and activity under alkaline conditions [75]. Since HEAs hold multi-element compositions, the interaction between multiple metal elements enhances the adsorption and desorption of intermediate species such as O*, OH*, OOH* [76], and H* [73], which are crucial to HER and OER catalytic performance. An optimal alloy composition is critical to the design of HEAs as it affects the formation of coordinated active catalytic sites [77]. The selection of components for HEA synthesis is a complex process that requires careful consideration of cost, availability, catalytic effectiveness, and miscibility of the individual elements.

Typical HEAs consist of four or more elements in proportions ranging from 5 to 35 at % [78] and, by far the most commonly used metals are Ni, Fe, and Co as shown in Fig. 5(a), which illustrates the prevalence of elements commonly reported in ED-HEAs for water electrolysis applications. Each bubble represents a distinct element with the bubble size indicating its relative popularity across various reported compositions (Table S2, cf. ESM). Mn, Cr, and Cu commonly appear as the 4th and/or 5th elements. The combination of various metals with different properties provides new or enhanced absorption sites on HEAs, leading to different catalytic pathways or improved conditions for existing reactions. In Fig. 5(a), the elements to the right have higher reduction potential ($E°$) under aqueous conditions and therefore are easier to reduce (or easier to electrodeposit) than those to the left. This diverse electrochemical behavior presents a challenge for achieving homogeneous ED with multiple elements. $E°$ will be discussed in detail in the sections dedicated to individual elements. The *Y*-axis of Fig. 5(a) shows the different atomic radii of the elements. It is observed that elements with relatively large radii, such as W, Mo, Zn, and Al, are also used, but to a lesser extent. The mixing of elements with varying atomic radii helps stabilize the solid-solution phase [79]. This atomic size mismatch also introduces lattice distortions, leading to significant lattice strain, as illustrated by

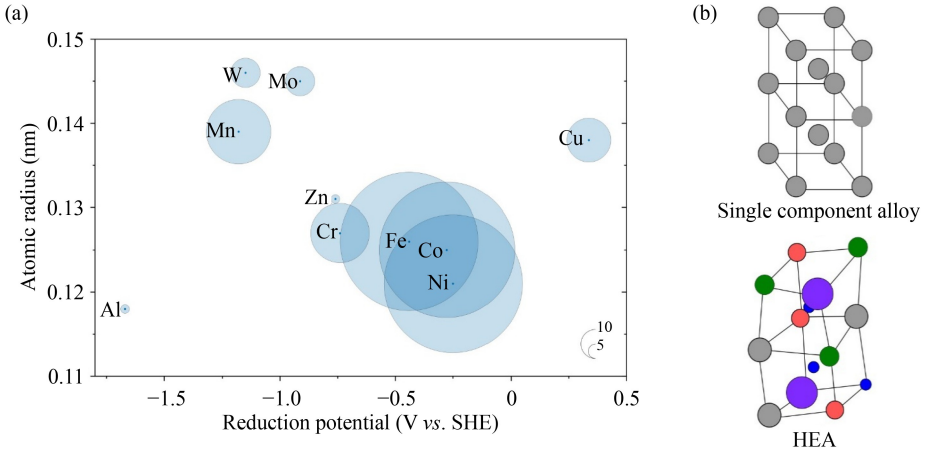

Fig. 5 (a) Bubble chart of non-noble elements in ED-HEAs with water splitting applications, by atomic radius and reduction potential; bubble size reflects their use in the reviewed literature as summarized in Table S2 (cf. ESM). (b) Schematic of a body-centered cubic structure comparing a traditional single-component alloy and a multi-component HEA, highlighting random atomic arrangement and lattice distortion.

Fig. 5(b) [80,81]. Such features influence the physical and chemical properties of HEAs and enhance their electrocatalytic performance by altering the binding energies of key reaction intermediates such as *H, *OH, and *O [82].

While Fig. 5(a) highlights the general trends in element selection, precisely understanding their role remains challenging due to the complex multi-element nature of HEAs, as well as the difficulty in achieving a uniform equiatomic structure. As the HEA field is still in its infancy, the long-term stability of HEAs in electrocatalytic environment is not yet well understood, especially in large-scale applications [83]. To gain a deeper understanding, the following sections will focus on the most frequently reported elements used in ED-HEAs for water-splitting applications. We will also examine their interactions during the ED process and their influences on the final alloy composition.

2.3.1 Nickel

Ni is known to perform exceptionally well at low current densities, and the synergistic benefits of NiFe and NiFeCo systems are well-documented for enhancing the activity and structural stability of electrocatalysts [84,85]. In contrast, Fe and Co exhibit enhanced performance at high current densities and high overpotentials, providing a broad spectrum of electrochemical activity [86]. Ni is considered almost indispensable in non-noble metal HEAs used for electrocatalysis [77]. It facilitates efficient charge carrier transport and increases the covalence of Fe–O and Co–O bonds, thereby promoting lattice oxygen as active sites and oxidation resistance [87−89]. Additionally, Ni enables the formation of NiOOH intermediates, which lowers the energy barrier and increases reaction rate [90,91]. In an electrolyte bath, the ED of Ni is influenced by the presence of Fe ions. Fe-induced inhibition of Ni reduction has been observed and attributed to the decrease in available free surface caused by the occupation of $Fe(OH)_2$ [92].

2.3.2 Iron

Similar to the competition of Fe with Ni in NiFeCoMn [92]. The same effect was reported in Fe with Cu during the ED of NiFeCoCuZn [93], resulting in increased Fe deposition in both cases. While Fe exhibited competition effect with Ni and Cu, it played an essential role in the ED of alloying elements such as W and Mo [94]. Studies indicated that Fe-group metals promoted the deposition of W and Mo by forming complex ions with these metals in the presence of citrate, a process known as co-deposition [61]. In addition, the plating rate of Fe has been reported to be accelerated by the presence of Co in the electrolyte bath [92]. Consequently, controlling the Fe content in the bath is essential for regulating the ED rate of these compounds. In terms of electrochemical activity, Fe has been shown to enhance OER activity of HEAs, as demonstrated in compositions such as FeCoNiCuMo [95], FeCoNiMn [86], and NiFeCoMnAl [91]. On the other hand, its presence in FeCoNiCuMo for HER in alkaline media hinder the surface adsorption of H* and desorption of hydrogen, ultimately reducing HER efficiency [95]. Despite this, Fe is consistently present in all reported ED-HEAs developed for HER applications. This apparent contradiction highlights a gap in understanding the specific role of Fe in non-noble metal-based HEAs during HER, revealing the need for further investigation.

2.3.3 Cobalt

The ED of NiCo containing alloys undergoes anomalous co-deposition in which an element with lower reduction potential (Co, $E°$ = –0.277 V) is more easily reduced than the one with higher reduction potential (Ni, $E°$ = –0.25 V), leading to Co enrichment. This phenomenon is attributed to the adsorption competition between metal hydroxides and metal ions, as the adsorption ability of $Co(OH)^+$ is greater than that of $Ni(OH)^+$ [96]. In multicomponent systems, ED of Co is favored at high current densities. Oliveira et al. [97] found that at higher currents Co content was increased, causing an amorphization of NiCoW-based alloys with negative impact on their corrosion resistance. The presence of Co in NiCo-based electrocatalysts could enhance the charge transfer process during the reaction, modify the electronic structure around Ni, and improve alloy conductivity [91,98]. Co was reported to increase the active ECSA of CoFeNiCrMnP [90] and FeCoNiCuMn [99] HEAs. This increase is attributed to the greater lattice distortion, as reported in studies on FeCoNiCuMn system [99].

2.3.4 Chromium

The incorporation of Cr in ED is often challenging due to its relatively negative $E°$, leading to low current efficiency and slow deposition rates. However, its successful incorporation into HEAs can significantly influence their structural and electrocatalytic properties. Its larger atomic radius compared to other alloying elements could increase the lattice constant of FeCoNiCr HEAs, contributing to lattice distortion and enhancing alloy stability [100]. Density functional theory calculations showed that CrO_x on HEA surface promoted the adsorption and dissociation of H_2O* and OH* species, enabled electronic interactions among metallic components, and activated other elements, such as Cu, as key sites for hydrogen (H*) adsorption [82]. Furthermore, Cr was observed to enhance electron transfer among Fe, Ni, Co, and improve HER performance of CoFeNiCrMn HEA [90]. For OER, Cr was found to accelerate the

process and improve catalytic performance of FeCoCrNi in alkaline electrolyte by regulating the valence states of Fe and Co ions, modifying the oxidation behavior of Ni and Co, and promoting the formation and stabilization of their active oxyhydroxide species [101]. In some cases, Cr has been shown to form a passivation layer to enhance corrosion resistance [68].

2.3.5 Copper

Opposite to Cr, the high positive reduction potential ($E°$ = + 0.337 V) of Cu represents a different challenge in ED-HEAs. Characterized by accelerated ED rate compared to other elements, over-deposition of Cu makes it difficult to achieve an equiatomic composition [93]. Therefore, Cu is often added to the electrolyte bath in lower concentrations relative to other elements to mitigate this issue. This cathodic behavior was also reported to enhance the corrosion resistance of coatings and their stability over time [87,102,103]. Additionally, Cu was prone to forming HEA dendritic structures with a high active surface area [104]. The electronic interactions between Cu and other metallic components could activate Cu as a key site for H* adsorption to enhance the HER performance of CoFeNiCrCu alloys [82]. In contrast, the influence of Cu on OER is more complex. Research on FeCoNiCuMo indicated that Cu remained relatively inert compared to other elements [95]. Therefore, controlling Cu content during ED can be delicate, depending on the HEA components and targeting reaction.

2.3.6 Manganese

The highly negative reduction potential of Mn poses challenges for its ED in aqueous solutions. To overcome this, additives such as ammonium sulfate are commonly recommended [105]. When included in electrocatalyst, Mn facilitates the self-construction of active NiOOH intermediates, thereby enhancing the regeneration of catalysts during operation [106]. Han et al. [91] identified Mn as an electron donor in NiFeCoMnAl HEAs, in which its low electronegativity could facilitate efficient electron transfer to Ni, Fe, and Co. This transfer increased the electron density around these acceptors and improved the electrocatalytic performance. Asghari et al. [107] observed lower charge transfer resistance in CoCuFeNiMn systems after addition of Mn. In FeCoNiMnW HEAs, Mn enhanced HER efficiency [94], and boosted OER performance in FeCoNiMn catalysts [86]. Dąbrowa et al. [108] provided a detailed analysis of the influence of Mn on HEAs, highlighting its significant contribution to the sluggish diffusion effect. Their study demonstrated that Mn-containing alloys exhibited lower diffusion coefficients compared to those without Mn. By incorporating Mn, the diffusion barriers are increased, leading to slower atomic movement within the alloy, which made Mn a great alloying element for HEAs when stability at elevated temperatures is required.

2.3.7 Tungsten

W cannot be electrodeposited independently with a tungstate-based aqueous solution. However, it can be incorporated into HEA coatings through an induced co-deposition mechanism in the presence of iron-group metals such as Co, Fe, or Ni [109]. This process involves an intermediate reaction between the tungstate anion and these metals [61]. A competition between W and Mo was reported in ED for NiMoW alloys with more Mo being deposited than W, although equimolar amounts of both were initially used [110]. To enhance the incorporation of W, conditions that promote citrate protonation and dechelation, such as lowering the pH and increasing the initial W concentration can be applied.

The incorporation of W is desired when catalyst stability is critical under the applied potentials for HER and OER catalysis. W could form a protective layer *in situ* during operation, thereby preventing catalyst degradation due to dissolution [94]. It also improved mechanical properties, including durability, hardness, and the resistance to high temperatures [111]. Due to its large atomic radii (0.141 nm), W is also known to induce significant structural changes in HEAs. Haché et al. [61] observed that the threshold content of W for a nanocrystalline-to-amorphous transition occurred between 9% and 11% in FeCoNiCuMo, with surface cracking at W content of 32 wt %. High-valence non-3d metals, such as W, can modify the adsorption energies of relevant OER intermediates at the active sites of 3d metals such as Co and Ni, leading to enhanced OER activities [112], which is supported by the superior OER activity of NiFeCuCoW HEA [113]. The inclusion of W in FeCoNiMnW alloys also resulted in enhanced HER efficiency [94]. W not only acts as a protective stabilizer but also contributes to enhanced HER and OER performance. ED is one of the few techniques that enables the straightforward incorporation of such high-melting-point elements into HEA systems.

2.3.8 Molybdenum

Similar to W, Mo must be deposited alongside Fe, Ni, or Co and is often used in the co-deposition of Mo-W alloys. Increasing the Mo concentration in the bath enriches the final alloy with Mo and Fe, while reducing the incorporation of Ni, Co, and W. Haché et al. [61] reported that a maximum achievable Mo + W content of approximately 30 at % resulted in brittle NiFeCoWMo deposits, making it challenging to achieve equiatomic compositions. As a high-valence metal, Mo facilitates rapid multi-electron transfer between species with various oxidation states, which improves catalytic intrinsic activity. It has shown

that incorporating Mo into HEAs significantly enhanced OER activity, and thus water electrolysis performance, by facilitating the electronic structure of FeCoNi alloy [114]. Cheng et al. [115] demonstrated that Mo reduced the OER overpotential of FeCoNiMo-OH [115]. Similarly, Mo was found to improve the OER performance of CoCuFeNiMo [107] and FeCoNiMoCr [116]. In the latter case, Mo addition also decreased the dissolution of Fe, Co, and Ni, enhancing its corrosion resistance. Mo improved HER catalytic performance in alkaline electrolyte by facilitating H_2O dissociation, reducing the energy barrier for electrochemical adsorption, and accelerating the chemical desorption process [95].

2.3.9 Zinc

The incorporation of Zn in HEAs for electrochemical applications is relatively uncommon due to the formation of poorly soluble Zn hydroxides, which impede the reduction of other metal ions by covering the cathode surface [117]. Reddy et al. [93] observed this issue during the ED of FeCoNiCuZn and mitigated it by lowering Zn concentration in the electrolyte bath. Although Zn itself is catalytically inactive, its performance can improve in the presence of Mo. Zn synergizes with Mo by modulating the levels of Mo^{4+} and Mo^{6+} and enhancing the distribution of high-valence ions. This interaction was found to promote the adsorption of OER intermediates and improve the overall catalytic performance of FeCoNiMoZn, while the addition of Zn alone had a negligible effect on the overpotential in FeCoNiZn, its combination with Mo led to a reduced OER overpotential [115]. Therefore, when Zn is included in the electrolyte bath, it should be maintained at low concentrations and preferably co-deposited with Mo to mitigate deposition challenges and promote synergistic effects that enhance OER performance.

2.3.10 Aluminum

Al is commonly utilized in surface engineering for dealloying to create nanoporous structures with increased surface and exposure of active sites [91]. Besides morphology, its incorporation can affect the structural characteristics of HEA coatings. For example, Aliyu et al. [102] observed that the incorporation of Al in AlCrFeCoNiCu HEA coatings increased the body-centered cubic phase through lattice distortion. In ED baths, $AlCl_3$ is commonly used as a source of Al ions and as a buffer in the electrolyte bath, especially when Cr^{3+} ions are in solution to stabilize pH and prevent Cr precipitation [118].

2.3.11 Phosphorus

P atoms could display metallic characteristics when integrated into the metal lattice at optimal ratios [119]. Their higher electronegativity compared to metal atoms enables them to pull electrons from the lattice [120]. The incorporation of P decreased crystal grain size in NiFeCoWP, leading to increased surface area and improved catalytic performance [121]. In HER, negatively charged P atoms effectively captured positively charged protons (H^+), thereby boosting HER performance [122]. The strain introduced by P atom can be tailored and used to influence alloy structure and thus the electronic structure of transition metal elements in HEAs, leading to increased activity for electrochemical water spitting [123].

2.4 Coating substrate

In ED, a conductive substrate provides a surface on which the HEA film can grow. A well-selected substrate can improve the uniformity of the deposited coating and enhance the conductivity of the electrode. While its role in the nucleation mechanism and growth process of conventional alloy films has been extensively investigated, the effect of the substrate on the final properties of ED-HEA films has not been studied in depth. Białostocka et al. [124] examined the ED of FeNi films on three different substrates, Cu, brass, and silver, and found significant variations in adhesion, crystalline structure, and composition of the resulting films. The variations in these characteristics can impact HEA films that have multiple elements involved during the ED process. A study investigating CoCrFeMnNi HEA films deposited on Cu and Al substrates revealed that films on Cu exhibited significantly higher corrosion resistance then those on Al [125]. The superior corrosion resistance of HEA/Cu systems could be attributed to both the optimized deposition process and the high reduction potential of Cu. In contrast, Al corrosion resistance depends on the formation of a passive oxide film, which is likely disrupted during the ED process.

Cu sheets are frequently used as substrate materials for ED-HEAs. Cu has high conductivity to promote uniform deposition and is an ideal platform for ED-HEAs due to its chemical stability [126,127]. HEAs such as NiFeCoWMo [29] and NiFeCoCr [101] were successfully deposited on pretreated Cu sheets [61,128]. More robust substrates, such as Fe and steel, are preferred in traditional cells for their mechanical strength and durability to support thicker HEA coatings [113]. Some limitations with metallic sheets are the low surface area and lack of porosity, which restrict their application in flow-through cells and zero-gap electrolyzers. These challenges can be addressed with porous and/or 3D substrates such as foams, felts, and cloths that provide higher surface area and improved mass transport. In this context, ED offers a unique advantage over other film preparation techniques, as it enables coating of complex morphologies and interconnected porous networks with

controlled composition. Cu foam has occasionally been used as a substrate, for example, in FeCoNiCuMn [99] and FeNiCoCrMn [129] HEAs. In contrast, Ni foam is among the most widely used substrates its high activity and stability toward both OER and HER [130]. It is commercially available and versatile in terms of specifications, and requires minimal pre-treatment, making it an ideal candidate for ED. Carbon-based supports, such as carbon paper [94] and carbon cloth [116], are also frequently used. These materials offer excellent conductivity, porosity, and cost-effectiveness. However, unlike Ni substrate they are inert to electrocatalytic processes [94,131].

Overall, the catalytic performance of HEAs is profoundly influenced by the synergistic effects within their multicomponent systems [132], including the interactions among individual elements and their specific roles. Composition, microstructure, surface properties, and electronic structure are the key factors that influence the electrocatalytic performance of HEAs. Therefore, strategies for tailoring these factors to enhance HEA performance are needed. Better understanding of HEA properties and structures can help optimization for specific applications through precise adjustments to achieve desired properties. Careful composition design and structure-property relationships are essential to unlocking the full potential of HEAs in advanced applications.

3 ED parameters

The effectiveness of ED process during the synthesis of HEAs is largely dependent on the control of composition, morphology, and properties of the resulting alloy coatings. The evolution and composition of the films are dictated by several factors, including the reduction potential of the elements present in the electrolyte, its pH value, concentrations of the elements in the bath, and complexing agents [62,93,133]. Additionally, precise control of parameters such as ED current, temperature, time, and stirring is also important to preventing segregation in multicomponent systems and optimizing alloy morphology and activity. Although ED has been extensively used for single-element and binary alloy films, incorporating multiple alloying elements and achieving a solid solution phase with near-equiatomic ratios remains challenging, which underlines the complexity of the process and the need for further research. It is suggested that lower-order systems (i.e., those containing three metals) be studied first in detail to fully understand how additional elements play a role in ED for HEAs. This progressive step-wise approach allows evaluation of the effect of these parameters on properties to establish a base understanding of the fabrication of bulk nanocrystalline HEAs [133]. Given that, Fig. 6 illustrates the ranges and frequencies of use of four key synthesis parameters (current density, temperature, time, and electrolyte pH) reported in the literature for ED-HEAs used in electrocatalytic water splitting. The size of the bubbles indicates how often each specific value on the Y-axis (parameter value) is used in these studies, highlighting a broad and somewhat arbitrary distribution. This variability in the reported values indicates the absence of a standardized method for optimizing synthesis conditions to achieve desired

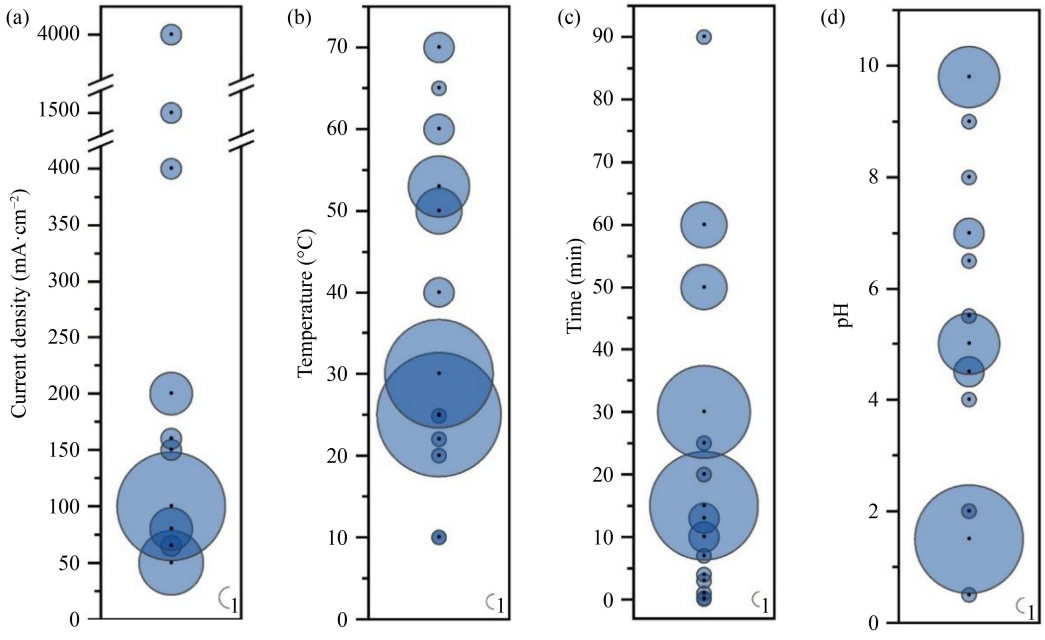

Fig. 6 Bubble chart depicting frequency of reported synthesis parameters for ED-HEAs used in water splitting: (a) current density, (b) temperature, (c) deposition time, and (d) electrolyte pH.

electrochemical properties. The following paragraphs discuss the findings from the literature on these key parameters and their impacts on HEA performance for electrocatalytic water splitting.

3.1 Bath compositopn

Baths are utilized in ED methods to create a "one-pot" solution that incorporates all the necessary ingredients for the synthesis of HEAs. Complexing agents, buffering agents, stress relievers, salts, and surfactants, are some of the ingredients used to tailor the synthesis of HEAs. The media can be aqueous, organic, or water-in-oil baths with each one having its advantages and disadvantages. Aqueous baths are the most used ones, in which deionized water is the solvent, and offer a cost-effective approach due to its environmental friendliness and easy accessibility. Their higher heat capacity compared to organic solvents makes them more thermally stable and safer for handling without concerns related to flammability and/or toxicity that other non-aqueous baths have. However, in certain cases baths with organic solvents may offer advantages such as enhanced solvating power to improve mass transfer of metal ions and achieve better adhesion and mechanical properties of HEA coatings [66].

Organic baths alleviate unwanted hydrogen evolution during ED, which can lead to the formation of porous structure to compromise coating uniformity and cause hydrogen embrittlement [98]. Typical organic solvents include mixtures of *N*,*N*-dimethylformamide and acetonitrile [134], or dimethyl sulfoxide and acetonitrile [135] often combined with metal chlorides (e.g., lithium perchlorate) to improve conductivity. Dense and uniform HEA films such as AlCrCuFeMnNi [134] and CoCrFeMnNi [135] have been successfully deposited using organic baths, forming spherical particles suitable for anti-corrosion applications. While less common in electrocatalysis, organic baths have shown promise for active high-surface-area HEA films. FeCoCrMnNi [136] and PtBiCoCuNi [32] HEAs were successfully deposited using organic systems and demonstrated high catalytic activity for OER and methanol oxidation, respectively.

Chloride, sulfate, or nitrate electrolyte salts are commonly used in aqueous, organic, or emulsified baths. While their direct impact on HEA properties has not been extensively studied, their selection is generally guided by solubility, availability, cost, and safety considerations. It is well-documented that introducing chloride ions increases the conductivity of the bath and improves the efficiency of the deposition process due to the non-interfering nature of the salt to the metal ions in solution [133].

Complexing agents (ligands) are often used to bring the reduction potentials of metals closer together, facilitating more controlled deposition [109]. This is particularly important for alloy co-deposition since it helps to balance the differing redox chemistry of metals in solution [61,137].

Including surfactants in the bath can help mitigate hydrogen bubble accumulation on the electrode surface, especially in the presence of Fe-based metal ions [133]. Sulphonic acid and surfactants such as sodium lauryl sulfate can refine grain structures by reducing surface tension and improving metal ion distribution at the cathode, resulting in a more uniform, stronger, and more corrosion-resistant coating [104]. Since hydrogen evolution is naturally present during aqueous ED, a buffer should be employed to stabilize the pH value. Boric acid, ammonium chloride, and other salt-based buffers can lower bath resistance and act as a pH buffers, preventing the formation of hydroxide layers that could hinder deposition. Stress releasers are sometimes used to enhance the deposition process by reducing the inherent stresses in electrodeposits caused by compounding mechanisms from atomic mismatching, impurity uptake, lattice defects, and crystalline joining, which can otherwise lead to cracking. Sodium saccharin slows down diffusion on electrode surfaces to favor nucleation over compounding growth [133,138].

Maintaining the initial equiatomic ratio becomes more challenging as the number of components in the bath increases due to their differences in $E°$. However, studies have shown that when water-in-oil emulsion systems are used, HEAs can be fabricated with similar atomic ratios to the solution ion concentrations. In this case, the emulsion creates a biphasic environment that allows reduction to occur immediately upon the collision of a water droplet with the electrode to form HEA with an almost equimolar composition [139,140]. When the nano-droplets are reduced to form individual nanoparticles on the substrate surface [141], films with fine-grained structures are formed due to the enhanced nucleation rate during deposition (Fig. 7).

3.2 Current density

Commonly used current density for ED-HEAs is typically in the 50 to 100 $mA \cdot cm^{-2}$ range, although higher current densities are occasionally used (Fig. 6(a)); direct, pulse, and cyclic current applications are the most utilized procedures. Pulse current (PC) offers a slight advantage over direct current (DC) because of its better current distribution and ion mass transfer to generate a more stable microstructure [142]. Figure S1 (cf. ESM) shows the distinct current profiles associated with each technique. DC generates a continuous electrical field over time, either as voltage or current, to create a constant negatively charged layer on the cathode surface. In contrast, PC intermittently interrupts the current flow to allow the charged layer to dissipate during the off periods. Cyclic voltammetry (CV) involves applying a

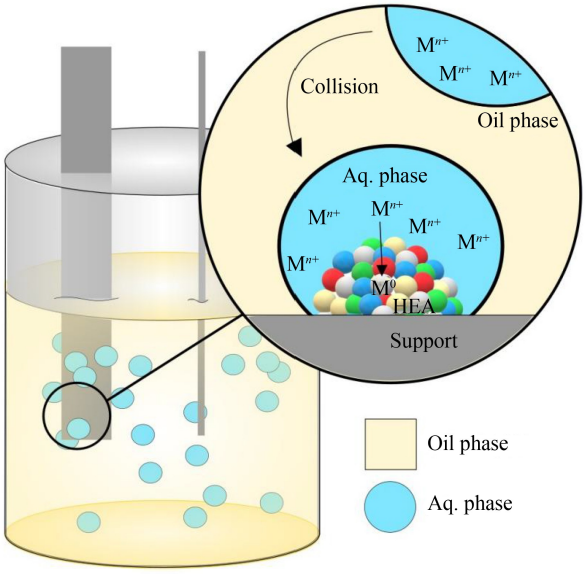

Fig. 7 Illustration water-in-oil experiment showing reduction of aqueous nano-droplets at electrode surface.

varying voltage in a cyclic manner.

HEA composition is influenced by the applied current density during the ED process and therefore it is important to understand the reduction potentials and electrochemical behavior of the different metal species in the bath. According to Aliyu et al. [102] for CuFeNiCoCr HEA system, alloying elements with high reduction potentials, such as Cu (+0.337 V), are primarily governed by the energy required to start the reaction on the electrode surface. In contrast, elements with low reduction potentials, like Cr (–0.74 V) are mainly influenced by diffusion, meaning that their deposition depends on how quickly they move through the solution to the electrode surface. They concluded that increasing the current density results in higher Cu incorporation, while Cr content decreases [102]. However, a different current-dependent behavior was observed for Cr in FeCoNiCr coatings in which Cr content increased, with increasing current density from 150 to 350 mA·cm^{-2}, likely due to the current overcoming its slow multi-step reduction kinetics ($Cr^{3+} \rightarrow Cr^{2+} \rightarrow Cr^{0}$) due to charge transfer limitation. The same study also found that Co content decreased with increasing current, possibly due to diffusion limitations at elevated current densities [100]. So, while reduction potential may indicate an initial ED behavior, the actual incorporation of each element also depends on its specific kinetic pathway, ion transport properties, bath composition, and the current range being evaluated.

In line with this, a recent study by Ahmadkhaniha et al. [143] observed that during the ED of NiCoWMoCu HEAs, Cu content initially decreased and then increased with current density, indicating initial suppression followed by improved charge transfer at higher currents. In contrast, W, Mo, and Co showed the opposite trend, suggesting a shift from charge transfer control to diffusion limitation. Ni content steadily increased due to its efficient reduction kinetics and high diffusivity. Additionally, oxygen incorporation declined at higher current densities, indicating more complete metal reduction and reduced formation of oxygenated species. Thus, selecting an appropriate current density for ED-HEA requires balancing the kinetic barriers of noble elements (e.g., Cu), the diffusion limitations of non-noble elements (e.g., Mo, W, Co), and the overpotential required to activate slow-reacting species like Cr.

Current density also impacts HEA surface morphology since it affects the nucleation and growth rates of the deposited films. At higher current densities, the increased cathodic polarization accelerates ion reactions and promotes more uniform nucleation. In contrast, at lower current densities, the deposition process is slower, resulting in uneven grain growth. Consistent with this behavior, FeCoNiCr films deposited at 300 mA·cm^{-2} exhibited better coating uniformity and a more equiatomic composition compared to those obtained at 150 mA·cm^{-2} [100]. Similarly, in FeCuCoW films, increasing the current density from 50 to 100 mA·cm^{-2} resulted in more compact particle clusters and a more uniform coating [113]. Increasing current density also resulted in greater film thickness, as observed by Xiao et al. [144] with CrMnFeCoNi films that were increased from 0.5 to 1.5 μm when the applied potential was raised from –2 to –3 V.

To achieve equiatomic compositions, Wang et al. [82] developed an innovative technique called far-from-equilibrium ED. This technique could rapidly alter the synthesis conditions by using a high-voltage cell with high current densities, creating a far-from-equilibrium state that narrows the reduction potential gap and promotes the formation of uniform HEAs from multiple cations. In this method, the typical potentials range from –8 to –16 V (–300 and –1500 mA·cm^{-2}) as illustrated in Fig. 8 [82].

For pulse ED, Reddy et al. [93] investigated the impact of duty cycles on ED for FeCoNiCuZn HEA films. Their findings revealed that deposits with a high Cu content

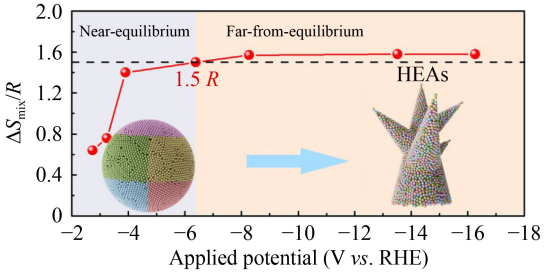

Fig. 8 Illustration of far-from-equilibrium electrosynthesis. Dependence of ΔS_{mix} of as-prepared samples on applied potential. Reprinted with permission from Ref. [82], copyright 2023, Chinese Society of Metals.

were achieved at lower duty cycles (< 0.75), whereas higher duty cycles (> 0.75) resulted in more balanced compositions across all five elements. Higher duty cycles facilitated the deposition of elements with higher anodic reduction potentials, such as Fe, Co, Ni, and Zn, thereby increasing their relative proportions in the deposits. Furthermore, surface coverage was improved with higher duty cycles. In contrast, lower duty cycles led to decreased surface coverage as the shorter time-on limited the amount of material that could be deposited.

Similarly, CV can control the deposition process through its ability to precisely regulate deposition through cyclic variations in applied potential. During the reduction step, ions reduction occurs, and the coating is formed. The oxidation step could further modify the double layer and the absorbed species on the surface. In addition, it could incorporate oxides onto the cathode and promote selective dissolution at the surface. The study by Nourmohammadi et al. [98] demonstrated that the number of CV cycles significantly impacted the uniformity of CuNiFeCoCr films. They found that approximately 25 CV cycles typically resulted in enhanced structural characteristics and more consistent coverage. Adjusting and optimizing the number of CV cycles can provide additional control over the deposition process.

3.3 Bath temperature

ED temperature reported in the literature ranges from 10 to 70 °C, with a strong preference for room temperature (25 °C) and nearby values, as shown in Fig. 6(b). Moderate temperatures (30–53 °C) are also commonly reported due to their benefits in enhancing ion mobility and deposit quality. Higher temperatures (above 60 °C) and very low temperatures (below 10 °C) are rarely used.

A suitable bath temperature can improve ED process stability, ion mobility, grain growth, and nucleation, resulting in increased deposition rates and smoother coatings [66]. Excessive temperatures can cause increased evaporation of the plating solution, which alters salt concentrations and effective cell volume. Too low temperatures reduce ion migration rates and salt solubility, leading to higher potential requirements. Santana et al. [145] demonstrated that increasing the bath temperature from 21.5 to 63.5 °C favored the deposition of Co over Ni in NiWCo alloys due to enhanced ion diffusion. Higher temperatures improved the diffusion of complex ions like tungstate and citrate, thus accelerating W deposition [146,147].

Guo et al. [100] found that when the bath temperature exceeded 30 °C, the Cr content in FeCoNiCr HEA coatings decreased, due to lower overpotential for hydrogen evolution at higher temperatures, which intensified HER and raised the local pH value. When the pH value exceeded 4.5, $[Cr(H_2O)_6]^{3+}$ complex underwent hydrolysis and formed high-molecular-weight polymers through hydroxyl-bridge polymerization. These polymers precipitated near the cathode, reducing the availability of Cr^{3+} ions and resulting in lower Cr content in the final alloy [148]. The bath temperature also impacted particle size during ED for FeCoNiCuMn HEAs, in which case the deposition temperature was decreased from 25 to 2 °C to cause particle size reduction from about 1 μm to less than 5 nm [99].

3.4 Deposition time

The duration of ED plays an important role in controlling particle size and film thickness in HEAs. Both excessively short and prolonged deposition times can have a negative impact on the quality of the films. A short ED period results in insufficient film thickness, making it easier for corrosive agents to penetrate and reach the substrate, whereas a prolonged ED period leads to loose and uneven surfaces with pores and cracks to create paths for corrosion [149], grain coarsening, and adhesion concerns [66].

As seen in Fig. 6(c), the ED times reported in the literature vary significantly, ranging from as short as 6 s to as long as 90 min. Shorter deposition time results in smaller particle sizes, which benefits catalytic applications. For example, FeCoNiCuMn HEAs prepared with ED times of 4, 5, 6, and 7 min showed that a 4-min deposition resulted in the smallest particle size and the highest HER/OER activity [99]. Similarly, nanoflower-structured CoNiFeMnPO films HEAs with shorter deposition times formed more compact and densely packed nanosheets [150].

Zheng et al. [32] investigated the growth mechanism of PtBiCoCuNi HEA. Scanning electron microscope (SEM) micrographs taken at intervals from 50 to 1800 s revealed significant morphological variations: spherical nanoparticles were formed initially and increased in size and porosity until a sheet-like nanostructures began to form at about 800 s after which the morphology was retained with time. Nucleation, growth, and selective leaching collectively drive the transition from initial spherical nanoparticles to nanostructured surfaces in the later phases. The precise control of ED time enables the tailoring of these morphological transformations to optimize the properties of HEAs for electrocatalytic applications.

3.5 pH value level

As shown in Fig. 6(d), electrolyte baths with pH values ranging from 0.5 to 9.8 are reported for ED-HEAs, with a notable focus on slightly acidic to neutral conditions. Higher pH values (⩾ 7) are less frequently used due to the reduced stability of metal ions in solution, as they tend to precipitate under alkaline conditions. The bath pH dictates reaction chemistry and influences which elements

can be deposited or precipitated or can form complexes. In some cases, it has a greater influence on HEA formation than current density and bath temperature [97]. The bath pH can affect nucleation behavior, microstructure, and chemical composition of the resulting coatings. It was observed that lowering the pH value reduced both current efficiency and the incorporation of elements with low reduction potentials due to the high concentration of protons, leading to a significant portion of the current being used for proton reduction or hydrogen gas formation at the cathode [102]. However, at high pH values, metal hydroxide ions could cause cracks on the alloy and thus would require the use of buffer solutions in the bath [66]. Reddy et al. [93] examined how bath pH values affected the composition and morphology of FeCoNiCuZn HEA films and found that lower pH values (0.5 and 1.5) favored the deposition of Cu. As pH values increased to 2.5, the quality of the HEA films improved, resulting in better film characteristics with a balanced composition. However, at higher pH values (3.5 and above), cracks were visible, which were attributed to the presence of OH^- ions that caused precipitation at the electrode-electrolyte interface. When the pH value reached 5 or higher, metal salts precipitated, causing instability and opacity in the electrolyte.

Another study investigated the effect of pH value on the elemental composition of electrodeposited NiWCo alloy and showed that raising the bath pH value led to a higher Ni content and a lower Co content [149]. At pH values between 2 and 5, the presence of $Co(OH)_2$ at the electrode/electrolyte interface promoted the reduction of Co due to competitive hydroxide adsorption, which favored the reduction of the element with the lower reduction potential. Conversely, at alkaline pH value levels, the decrease in $Co(OH)_2$ and increase in $Ni(OH)_2$ shifted the preference toward Ni reduction [97]. Similarly, Carroll et al. [29] observed a decrease in Co concentration as the pH increased from 5 to 6 during the ED of NiFeCoMoW HEAs. They also reported unpredictable variations in Ni and Fe content with changes in pH, whereas Mo and W remained relatively stable. It is evident that the pH value of the electrolytic bath plays an important role in determining the quality, composition, and catalytic properties of ED-HEAs. It strongly influences ion stability, film uniformity, and deposition mechanisms during ED. However, these impacts remain unpredictable, showing the need for deeper investigation.

3.6 Agitation

Agitation during ED plays a pivotal role in achieving uniform coatings by maintaining consistent electrolyte concentration at the electrode surface. It enhances mass transfer of ions from the bulk solution to the electrode surface, reduces concentration polarization, and promotes film nucleation and growth [151]. In multicomponent systems like HEAs, the effective stirring of the electrolyte is essential due to the complexity of the bath and multi-element interactions. Stirring also facilitates the mixing of metal salts and additives, which increases the stability of electrolyte. In addition, it helps remove gas bubbles from the electrode surface generated during the ED process, preventing pit formation in the coatings [102]. The stirring speeds reported in the literature for ED-HEAs appear arbitrary, ranging from 0 to 850 $r \cdot min^{-1}$, with most studies using moderate stirring around 250 $r \cdot min^{-1}$. Interestingly, stirring speed is often omitted or overlooked in reporting experimental work. Future research should include this factor to establish more consistent and standardized guidelines.

Agitation can be achieved by magnetic stirring, rotating disk electrodes (RDE), nitrogen bubbling, or ultrasonic agitation, among which magnetic stirring and RDE are the most widely used. Each method offers distinct advantages depending on the specific deposition conditions and objectives. RDE provides precise control of hydrodynamic conditions through a uniform laminar flow [152], making it ideal for achieving high reproducibility [153]. However, edge effects with RDE can cause element enrichment at the disk perimeter. Huang et al. [92] reported increased Ni and decreased Co content during FeCoNiCu ED at the disk perimeter. Magnetic stirring, on the other hand, is simple, cost-effective, but less precise. It generates a turbulent flow throughout the electrolyte, enhancing mass transfer during ED and increasing current efficiency [154].

Hadipour and Bharololoom [154] found that magnetic stirring produced Ni coatings with higher current efficiency and surface roughness than those from RDE. Other studies on Ni ED have shown that increasing agitation decreases the deposition rate, crystallite size, and lattice strain, and improves uniformity and corrosion resistance [155]. However, excessive stirring introduced surface bubbles and affected coating quality [156], indicating that an optimal stirring rate is necessary for property control. In binary coatings, stirring alters deposit composition by enhancing ion transport and affecting which metals are preferentially deposited. For example, in Co-Ni coatings, Co content increased with RDE speed. In Fe-Ni coatings, stirring enhanced Fe incorporation at high current density (700 $mA \cdot cm^{-2}$), consistent with anomalous ED under diffusion control. In contrast, at lower current density (50 $mA \cdot cm^{-2}$), Ni content increased with stirring speed [157]. For Cu-Co alloys, stirring increased Cu content [158]. These results indicate that stirring favors the deposition of the more transport-limited ion. The only study on a five-component NiFeCoWP alloy was conducted by Bachvarov et al. [121] who compared coatings formed with and without stirring, they observed that stirring decreased Ni content and increased Co and Fe contents. Similar to binary

systems, the composition of multicomponent coatings can also be tuned by adjusting stirring conditions.

3.7 Nanostructured electrodeposited HEA films

The structural and functional properties of HEA films are also influenced by film thickness and morphology, which are often underreported in published studies. Film thickness determines mechanical integrity, stability, and adhesion. Significant variability in film thickness has been reported, ranging from ultrathin films (5 nm) for NiFeCoMoCrOOH [116], through intermediate films between 3 and 5 μm for NiFeCoCrCu [159], to thick coatings of up to 100 μm for NiFeCoCrMn [125]. In some cases, film characteristics were reported in terms of mass per unit area, such as NiFeCoMnCu films at 19.8 mg·cm^{-2} [99], reflecting inconsistency in reporting standards.

High temperatures and prolonged deposition times result in increased film thickness. The incorporation of elements with high $E°$, such as Cu, enhances the current efficiency of the ED process and therefore promotes the formation of thicker coatings.

Film morphology directly influences the active surface area, thus the catalytic activity and overall catalyst functionality. ED-HEAs can exhibit diverse morphologies in two key metrics: double-layer capacitance (C_{dl}) and ECSA. C_{dl} is used as an indirect indicator of the surface area, which incorporates the capacitance associated with the charge stored in the electrical double layer at the electrode-electrolyte interface. A higher value of C_{dl} indicates a higher surface area. ECSA can be calculated by the following equation:

$$\mathrm{ECSA} = \frac{C_{dl}}{C_s}, \tag{4}$$

where C_s is the specific capacitance of a smooth standard electrode, which is approximately 0.022 mF·cm^{-2} for a flat electrode.

Figure 9 reveals some selected SEM images reported for ED-HEAs. A typical morphology observed is the globular structure (Fig. 9(a)), characterized by spherical particles. These are typically formed under diffusion-controlled conditions due to metal ion depletion near the cathode caused by low ion concentration or insufficient stirring [93]. When nucleation dominates over particle growth during ED, smaller particles are formed, resulting in granular morphologies that appear as aggregated nanoparticles or microparticles, either spherical or irregular. For example, FeCoCrMnNi HEAs exhibited nano-sized particles with a C_{dl} of 7.87 mF·cm^{-2} [136], whereas FeNiCoCrMn HEAs showed fine particles with a C_{dl} of 32.9 mF·cm^{-2} (Fig. 9(b)) [129]. Recently, Liu et al. [74] achieved ultra-fine particles with a dense nanoscale micro-convex stacking morphology for FeNiCoCrMn HEAs, referred to as 'raspberry-like' films (Fig. 9(c)). These structures had exceptionally high surface areas and C_{dl} of 190.63 mF·cm^{-2}, and one of the lowest reported HER overpotentials. Some elements, such as W, Mo, Cr, Zn, and Al, may dissolve into electrolyte, which can create pores and increase ECSA in alkaline OER conditions [91,160].

The addition of Cu to HEAs could promote dendritic (Fig. 9(e)) or cauliflower-like (Fig. 9(d)) morphologies

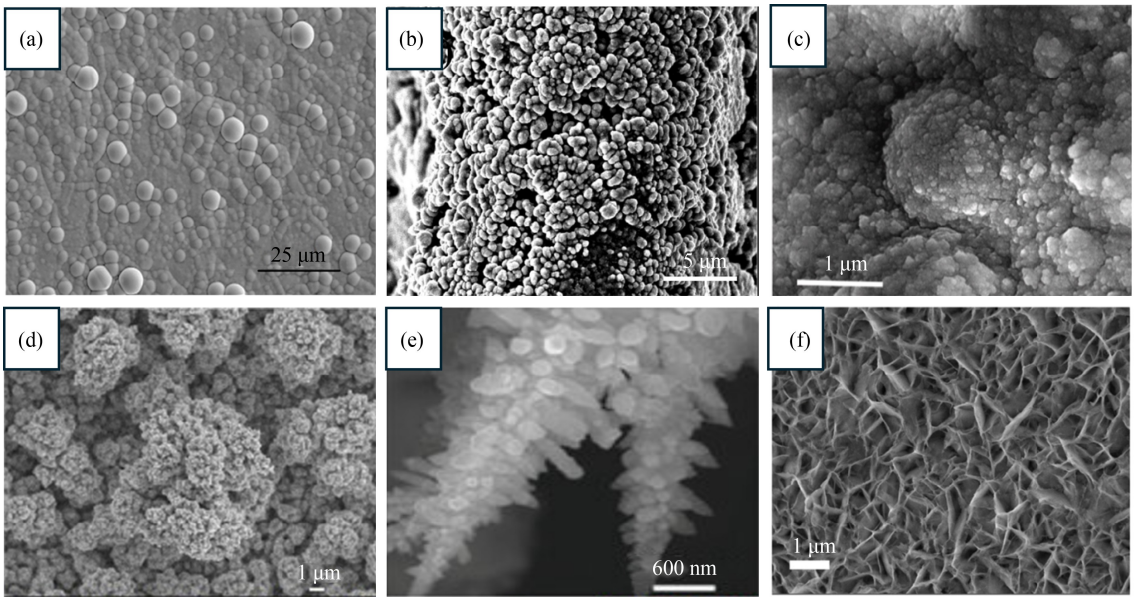

Fig. 9 SEM images of (a) globular NiFeCoCr. Reprinted from Ref. [128], copyright 2023, the Author(s). (b) Ultra-fine particles FeNiCoCrMn. Reprinted with permission from Ref. [129], copyright 2024, Elsevier. (c) 'Raspberry-like' FeNiCoMnV. Reprinted with permission from Ref. [74], copyright 2024, Elsevier. (d) 'Cauliflower-like' NiFeCoWCu. Reprinted with permission from Ref. [113], copyright 2023, Elsevier. (e) Dendritic NiFeCoCrCu. Reprinted with permission from Ref. [82], copyright 2023, Chinese Society of Metals. (f) Nanosheets NiFeCoMoZn. Reprinted from Ref. [115], copyright 2024, the Author(s).

depending on the current density. At high current density, NiFeCoCrCu alloys exhibited dendritic tree-like formations driven by hydrogen evolution with a C_{dl} value of 10.2 mF·cm^{-2} [82]. Conversely, at lower current density more controlled cauliflower-like structures were favored. Alloys such as NiFeCoMnCu, NiFeCoWCu, and NiFeCoCuMo exhibited such morphologies [87,95,113], which was believed to enhance active sites and expand the contact area [149,161]. Nanosheet morphologies (Fig. 9(f)) are also commonly reported in HEAs and conventional LE systems, which provide a high surface area to benefit catalytic activity, as reported for CoFeNiCrMnP HEA with a high C_{dl} of 73 mF·cm^{-2} [90]. The formation of nanosheets is generally attributed to nucleation and growth under high current densities [162].

In an attempt to compare ED-HEA catalysts with other catalysts, we examined the roughness factor (R_f) values reported in the literature. R_f corresponds to the ratio of ECSA to its geometric area and reflects how much of the catalyst surface is electrochemically accessible relative to the electrode size [29]. For high and medium entropy materials, R_f values show a wide range from 23 to 538 cm^2·cm^{-2}geo, with one alloy reaching more than 2000 cm^2·cm^{-2}geo. The synthesis method strongly influences these values; ED-HEAs typically show higher R_f due to their porous and irregular morphologies, while oxides prepared by sol gel or microwave methods generally yield lower R_f [29,74,163,164]. Conventional catalysts, including NiCo@NC systems with R_f ranging from 112 to 504 cm^2·cm^{-2}geo [165] and other alloys such as NiMo, CoMo, and Co with a R_f values between 15 and 143 cm^2·cm^{-2}geo [29,166], such catalysts typically fall in a moderate range. Finally, Ir-based catalysts stand out with some of the highest R_f values reported, reaching 643 for Ir containing catalysts and exceeding 2000 for MnIr oxides [167]. The R_f of ED-HEAs vary widely and depends strongly on deposition parameters and composition. Optimization of synthesis conditions is crucial for achieving the desired surface area. However, we note that comparisons across studies should be made with caution, since not many studies report the R_f. We encourage that when reporting ECSA, values should be normalized by geometric area.

ED offers a versatile and simple route to engineer nanostructured HEAs with high surface area, which is critical for optimizing electrocatalytic performance for HER and OER. However, inconsistent reporting of C_{dl}, ECSA, and film thickness makes meaningful comparisons between studies difficult, limiting progress in the rational design of high-performance ED-HEA catalysts.

4 Research outlook

Despite ED-HEAs promising potential as electrocatalysts, some key areas of interest need to be addressed in future studies as current literature has largely focused on evaluating and enhancing their performance and less on degradation mechanisms and improvement of long-term stability. Fan et al. [168] make some suggestions to address these shortcomings in the field, namely charge and mass transfer effects, and long-term durability. Mass transfer is highly hindered due to bubble formation during water splitting, it reduces performance by blocking active sites and slowing ion/charge interactions, therefore, improving catalyst fabrication to promote detachment of gas bubbles can overcome this limitation and accelerate mass transfer. Structural degradation is another aspect of concern which makes their commercial viability challenging. Here, *in situ* characterization can play an important role and delineate degradation mechanisms, including phase transitions, morphology changes, and elemental leaching, to help improve long-term stability. The stability of electrocatalysts under high current densities does remain challenging and presents opportunities in the research field for further investigation and attention, especially toward industrial applications [169]. We suggest that HEAs be scrutinized as conventional electrocatalysts to focus on destabilizing factors from characterization data under various testing environments. Environments should include long-term testing of the HEA electrocatalysts under high current densities in alkaline and acidic electrolyte. Data stemming from such experiments will help illuminate some of the fundamental challenges exhibited by HEAs for water splitting applications and bridge the gap between laboratory and industrial scale development.

Several factors will be critical for successful translation to practical applications, including: (1) maintaining uniform coating morphology and composition across larger electrode areas, which may require optimization of bath hydrodynamics and current distribution; (2) electrolyte management, since ion concentration shifts, pH gradients, and byproduct accumulation become more significant in large-volume baths; (3) scalability of electrode substrates, where adhesion and mechanical stability of HEA coatings are crucial for long-term operation; (4) cost-effectiveness and sustainability of precursors, which must be considered for industrial-scale ED. Addressing these factors will be essential to bridge laboratory developments with industrial electrolysis devices.

5 Conclusions

The unique combination of elements in HEA can lead to novel properties that can offer several benefits compared conventional catalyst materials. Benefits include tunable electronic properties and enhanced stability. Synergistic effects between constituent elements can lead to enhanced

catalytic activity and durability, although these linkages are still being investigated and general trends are being developed. On the same token, the degree of tunability can make it challenging to predict and even optimize such properties for specific applications. Normally, structure-property relationships are illuminated via repeated processes, theorical approaches and even trial-and-error, however, for HEAs, this is still being established. In addition, HEAs are still susceptible to corrosion in harsh electrochemical environments, which could potentially limit their long-term durability. Thus, more research is needed to fully understand and overcome these limitations. Unlocking the full potential of HEAs in water splitting and other catalytic applications has yet to be realized.

The synthesis of HEAs through ED offers immense potential for advancing electrocatalytic materials. This review demonstrates that the synthesis of highly active HEA films with excellent stability and enhanced nanostructured surface areas is feasible via ED, a simple and efficient method. ED for HEA preparation allows for precise adjustment of parameters, including current density, pH, temperature, stirring rate, and deposition time, providing the flexibility for a tailored design of HEA structures and compositions. However, the complexity of multi-component HEAs makes them sensitive and vulnerable in their structures to subtle variations in deposition conditions, posing challenges for reproducibility and standardization. Co-deposition of multiple metal ions may introduce competing reduction kinetics, preferential adsorption, and localized compositional variations that influence the uniformity, stoichiometry, and crystallographic properties of HEAs, leading to performance inconsistencies. Therefore, it is necessary and important to consistently report all ED parameters, including the often-overlooked factors such as stirring rate and film thickness, as well as clear rationales for synthesis conditions. We hope this review can help advance the understanding of the ED process for HEA synthesis to achieve optimization of HEA properties and performance as an electrocatalyst. While laboratory-scale studies have demonstrated promising results, reproducibility studies and medium to large-scale production of ED-HEAs with consistent properties remain underexplored.

Future research should prioritize unraveling the multi-element interactions in HEAs through integrated experimental and theoretical approaches. Advanced *in situ* techniques can provide deep insights into the dynamic processes during ED. Computational modeling can further elucidate ion reduction mechanisms, nucleation behaviors, and material microstructure evolution. Systematic studies on the effects of ED parameters can help establish clearer relationships between deposition conditions and HEA performance. By addressing these challenges and refining ED techniques for larger-scale applications, HEAs can be utilized to achieve their full potential as game-changing materials for sustainable energy solutions.

Competing interests The authors declare that they have no competing interests.

Acknowledgements The authors would like to acknowledge the Natural Resources Canada and the Government of Canada's interdepartmental Program of Energy Research and Development (PERD) managed by the Office of Energy Research and Development (OERD), for funding the study. We sincerely appreciate Dr. Hosnay Mobarok for his valuable comments and suggestions on revising the manuscript.

Electronic Supplementary Material Supplementary material is available in the online version of this article at https://doi.org/10.1007/s11705-026-2627-9 and is accessible for authorized users.

Funding Note Open access funding provided by Natural Resources Canada library.

References

1. George E P, Raabe D, Ritchie R O. High-entropy alloys. Nature Reviews Materials, 2019, 4(8): 515–534
2. Yu M, Wang K, Vredenburg H. Insights into low-carbon hydrogen production methods: green, blue, and aqua hydrogen. International Journal of Hydrogen Energy, 2021, 46(41): 21261–21273
3. Amini Horri B, Ozcan H. Green hydrogen production by water electrolysis: current status and challenges. Current Opinion in Green and Sustainable Chemistry, 2024, 47: 100932
4. Sadik-Zada E R. Political economy of green hydrogen rollout: a global perspective. Sustainability, 2021, 13(23): 13464
5. Wang S, Lu A, Zhong C J. Hydrogen production from water electrolysis: role of catalysts. Nano Convergence, 2021, 8(1): 4
6. Suermann M, Takanohashi K, Lamibrac A, Schmidt T J, Büchi F N. Influence of operating conditions and material properties on the mass transport losses of polymer electrolyte water electrolysis. Journal of the Electrochemical Society, 2017, 164(9): F973–F980
7. Zhang Q, Li Y, Luo F, Yang Z. Navigating the energy crisis: design principles and challenge in the development of high-performance catalysts for electrolytic water splitting. Chemical Communications, 2025, 61(58): 10747–10763
8. Priya K, Sathishkumar K, Rajasekar N. A comprehensive review on parameter estimation techniques for proton exchange

membrane fuel cell modelling. Renewable & Sustainable Energy Reviews, 2018, 93: 121–144

9. Barros R L G, Kelleners M H, van Bemmel L, van der Leegte T V, van der Schaaf J, de Groot M T. Elucidating the increased ohmic resistances in zero-gap alkaline water electrolysis. Electrochimica Acta, 2024, 507: 145161
10. Li W, Liu Y, Azam A, Liu Y, Yang J, Wang D, Sorrell C C, Zhao C, Li S. Unlocking efficiency: minimizing energy loss in electrocatalysts for water splitting. Advanced Materials, 2024, 36(42): 2404658
11. Schmidt G, Suermann M, Bensmann B, Hanke-Rauschenbach R, Neuweiler I. Modeling overpotentials related to mass transport through porous transport layers of PEM water electrolysis cells. Journal of the Electrochemical Society, 2020, 167(11): 114511
12. Xin Y, Li S, Qian Y, Zhu W, Yuan H, Jiang P, Guo R, Wang L. High-entropy alloys as a platform for catalysis: progress, challenges, and opportunities. ACS Catalysis, 2020, 10(19): 11280–11306
13. Nakaya Y, Furukawa S. Catalysis of alloys: classification, principles, and design for a variety of materials and reactions. Chemical Reviews, 2023, 123(9): 5859–5947
14. Suryanto B H R, Wang Y, Hocking R K, Adamson W, Zhao C. Overall electrochemical splitting of water at the heterogeneous interface of nickel and iron oxide. Nature Communications, 2019, 10(1): 5599
15. Du M, Lv X, Cao Z, Wang Q, Qu J. Review of catalytic electrodes containing iron-cobalt-nickel composite components for water electrolysis. ChemPhysChem, 2025, 26(3): e202400500
16. Huner B, Demir N, Kaya M F. Hydrogen evolution reaction performance of Ni-Co-coated graphene-based 3D printed electrodes. ACS Omega, 2023, 8(6): 5958–5974
17. Huo L, Jin C, Jiang K, Bao Q, Hu Z, Chu J. Applications of nickel-based electrocatalysts for hydrogen evolution reaction. Advanced Energy and Sustainability Research, 2022, 3(4): 2100189
18. Liu J, Du Y, Zheng D, Wang S, Hou Y, Zhang J, Lu X F. Nickel-based anode electrocatalysts for hydrogen production. ACS Materials Letters, 2024, 6(2): 466–481
19. Mehta A, Sohn Y. High entropy and sluggish diffusion 'core' effects in senary FCC Al-Co-Cr-Fe-Ni-Mn alloys. ACS Combinatorial Science, 2020, 22(12): 757–767
20. Kamaruddin H, Zhang J, Yu L, Wei Y, Huang Y. A review of noble metal-free high entropy alloys for water splitting applications. Journal of Materials Chemistry A: Materials for Energy and Sustainability, 2024, 12(17): 9933–9961
21. Carroll R, Lee C, Tsai C W, Yeh J W, Antonaglia J, Brinkman B A W, LeBlanc M, Xie X, Chen S, Liaw P K, et al. Experiments and model for serration statistics in low-entropy, medium-entropy, and high-entropy alloys. Scientific Reports, 2015, 5(1): 16997
22. Yeh J W. US patent, 2002159914A1, 2000-11-07
23. Ding J, Inoue A, Han Y, Kong F L, Zhu S L, Wang Z, Shalaan E, Al-Marzouki F. High entropy effect on structure and properties of (Fe,Co,Ni,Cr)-B amorphous alloys. Journal of Alloys and Compounds, 2017, 696: 345–352
24. Mu R, Wang Y, Niu S, Sun K, Yang Z. Wetting of $FeCoCrNiTi_{0.2}$ high entropy alloy on the (HfZrTiTaNb)C high entropy ceramic. Journal of the European Ceramic Society, 2023, 43(16): 7263–7272
25. Qiu Y, Thomas S, Gibson M A, Fraser H L, Birbilis N. Corrosion of high entropy alloys. NPJ Materials Degradation, 2017, 1(1): 15
26. Wu W H, Yang C C, Yeh L. Industrial development of high-entropy alloys. Annales de Chimie-Science des materiaux, 2006, 31(6): 737–747
27. Qin Y C, Wang F Q, Wang X M, Wang M W, Zhang W L, An W K, Wang X P, Ren Y L, Zheng X, Lv D C, et al. Noble metal-based high-entropy alloys as advanced electrocatalysts for energy conversion. Rare Metals, 2021, 40(9): 2354–2368
28. Choi S, Kwon J, Park C, Park K, Park H B, Paik U, Song T. FeCoNiCuIr high-entropy alloy catalysts for hydrogen evolution reactions with improved desorption behavior by tuning antibonding orbital filling. Energy & Fuels, 2023, 37(23): 18128–18136
29. Carroll Z L, Haché M J R, Wang B, Chen L, Wu S, Erb U, Thorpe S, Zou Y. Electrodeposited NiFeCoMoW high-entropy alloys with nanoscale amorphous structure as effective hydrogen evolution electrocatalysts. ACS Applied Energy Materials, 2024, 7(19): 8412–8422
30. Li P, Yao Y, Ouyang W, Liu Z, Yin H, Wang D. A stable oxygen evolution splitting electrocatalysts high entropy alloy FeCoNiMnMo in simulated seawater. Journal of Materials Science and Technology, 2023, 138: 29–35
31. Li P, Wan X, Su J, Liu W, Guo Y, Yin H, Wang D. A single-phase FeCoNiMnMo high-entropy alloy oxygen evolution anode working in alkaline solution for over 1000 h. ACS Catalysis, 2022, 12(19): 11667–11674
32. Zheng J, Li Y, Xu W, Sun B, Xu T, Liu S, Zhu X, Liu Y, Zhang S, Ge M, et al. Growth modulation of high-entropy alloys for electrocatalytic methanol oxidation reaction. Inorganic Chemistry, 2024, 63(43): 20697–20704
33. Pedersen J K, Batchelor T A A, Bagger A, Rossmeisl J. High-entropy alloys as catalysts for the CO_2 and CO reduction reactions. ACS Catalysis, 2020, 10(3): 2169–2176
34. Nellaiappan S, Katiyar N K, Kumar R, Parui A, Malviya K D, Pradeep K G, Singh A K, Sharma S, Tiwary C S, Biswas K. High-entropy alloys as catalysts for the CO_2 and CO reduction reactions: experimental realization. ACS Catalysis, 2020, 10(6): 3658–3663
35. Qi L, Guan J. Electronic structure modulation of high entropy materials for advanced electrocatalysis. Green Energy & Environment, 2025, 10(5): 917–936
36. Chen Z, Wen J, Wang C, Kang X. Convex cube-shaped $Pt_{34}Fe_5Ni_{20}Cu_{31}Mo_9Ru$ high entropy alloy catalysts toward high-performance multifunctional electrocatalysis. Small, 2022, 18(45): 2204255
37. Zhang G, Ming K, Kang J, Huang Q, Zhang Z, Zheng X, Bi X. High entropy alloy as a highly active and stable electrocatalyst for hydrogen evolution reaction. Electrochimica Acta, 2018, 279: 19–23
38. Zhu H, Sun S, Hao J, Zhuang Z, Zhang S, Wang T, Kang Q, Lu

S, Wang X, Lai F, et al. A high-entropy atomic environment converts inactive to active sites for electrocatalysis. Energy & Environmental Science, 2023, 16(2): 619–628

39. Yuan G, Wu M, Ruiz Pestana L. Density functional theory-machine learning characterization of the adsorption energy of oxygen intermediates on high-entropy alloys made of earth-abundant metals. Journal of Physical Chemistry C, 2023, 127(32): 15809–15818
40. Yang P, Jiang Z, Shi Y, Ren X, Liang L, Shao Q, Zhu K. Enhancement of oxygen evolution reaction performance of FeCoNiCrMn high entropy alloy thin film electrodes through in-situ reconstruction. Journal of Alloys and Compounds, 2023, 947: 169699
41. Ahmad A, Nairan A, Feng Z, Zheng R, Bai Y, Khan U, Gao J. Unlocking the potential of high entropy alloys in electrochemical water splitting: a review. Small, 2024, 20(29): 2311929
42. Li P, Wu B, Du K, Liu Z, Gao E, Yin H, Wang D. Highly stable single-phase $FeCoNiMn_X$ (X = Cr, Mo, W) high-entropy alloy catalysts with submicrometer size for efficient oxygen evolution. ACS Sustainable Chemistry & Engineering, 2023, 11(38): 14246–14254
43. Hao J, Zhuang Z, Cao K, Gao G, Wang C, Lai F, Lu S, Ma P, Dong W, Liu T, et al. Unraveling the electronegativity-dominated intermediate adsorption on high-entropy alloy electrocatalysts. Nature Communications, 2022, 13(1): 2662
44. Shi Y, Yang B, Liaw P K. Corrosion-resistant high-entropy alloys: a review. Metals, 2017, 7(2): 43
45. Shuang S, Ding Z Y, Chung D, Shi S Q, Yang Y. Corrosion resistant nanostructured eutectic high entropy alloy. Corrosion Science, 2020, 164: 108315
46. Quiambao K F, McDonnell S J, Schreiber D K, Gerard A Y, Freedy K M, Lu P, Saal J E, Frankel G S, Scully J R. Passivation of a corrosion resistant high entropy alloy in non-oxidizing sulfate solutions. Acta Materialia, 2019, 164: 362–376
47. Zhao Y, Wu J, Cao X, Li D, Huang P, Gao H, Gu Q, Zhang J, Wang G, Liu H. High-entropy materials for water splitting: an atomic nanoengineering approach to sustainable hydrogen production. Advanced Materials, 2025, 37(36): 2506117
48. Zhang T, Zhao H F, Chen Z J, Yang Q, Gao N, Li L, Luo N, Zheng J, Bao S D, Peng J, et al. High-entropy alloy enables multi-path electron synergism and lattice oxygen activation for enhanced oxygen evolution activity. Nature Communications, 2025, 16(1): 3327
49. Huang K, Xia J, Lu Y, Zhang B, Shi W, Cao X, Zhang X, Woods L M, Han C, Chen C, et al. Self-reconstructed spinel surface structure enabling the long-term stable hydrogen evolution reaction/oxygen evolution reaction efficiency of FeCoNiRu high-entropy alloyed electrocatalyst. Advanced Science, 2023, 10(14): 2300094
50. Wu J, Wang H, Liu N, Jia B, Zheng J. High-entropy materials in electrocatalysis: understanding, design, and development. Small, 2024, 20(43): 2403162
51. Zhou Q, Liao L, Zhou H, Li D, Tang D, Yu F. Innovative strategies in design of transition metal-based catalysts for large-current-density alkaline water/seawater electrolysis. Materials Today Physics, 2022, 26: 100727
52. Nørskov J K, Bligaard T, Logadottir A, Kitchin J, Chen J G, Pandelov S, Stimming U. Trends in the exchange current for hydrogen evolution. Journal of the Electrochemical Society, 2005, 152(3): J23
53. Li C, Baek J B. Recent advances in noble metal (Pt, Ru, and Ir)-based electrocatalysts for efficient hydrogen evolution reaction. ACS Omega, 2020, 5(1): 31–40
54. Chen Z W, Li J, Ou P, Huang J E, Wen Z, Chen L, Yao X, Cai G, Yang C C, Singh C V, et al. Unusual sabatier principle on high entropy alloy catalysts for hydrogen evolution reactions. Nature Communications, 2024, 15(1): 359
55. Wang B, Liu W, Leng Y, Yu X, Wang C, Hu L, Zhu X, Wu C, Yao Y, Zou Z. Strain engineering of high-entropy alloy catalysts for electrocatalytic water splitting. iScience, 2023, 26(4): 106326
56. Yeh C H, Hsu W D, Liu B H, Yang C S, Kuan C Y, Chang Y C, Huang K S, Jhang S S, Lu C Y, Liaw P K, et al. Low-frequency conductivity of low wear high-entropy alloys. Nature Communications, 2024, 15(1): 4554
57. Kumar A, Mucalo M, Bolzoni L, Li Y, Qu Y, Yang F. Facile synthesis of a NiMnFeCrCu high entropy alloy for electrocatalytic oxygen evolution reactions. Materials Today Sustainability, 2023, 22: 100360
58. Lone N F, Czerwinski F, Chen D. Present challenges in development of lightweight high entropy alloys: a review. Applied Materials Today, 2024, 39: 102296
59. Caramarin S, Badea I C, Mosinoiu L F, Mitrica D, Serban B A, Vitan N, Cursaru L M, Pogrebnjak A. Structural particularities, prediction, and synthesis methods in high-entropy alloys. Applied Sciences, 2024, 14(17): 7576
60. Haché M J, Zou Y, Erb U. Thermal stability of electrodeposited nanostructured high-entropy alloys. Surface and Coatings Technology, 2024, 482: 130719
61. Haché M J, Tam J, Erb U, Zou Y. Electrodeposited NiFeCo-(Mo, W) high-entropy alloys with nanocrystalline and amorphous structures. Journal of Alloys and Compounds, 2023, 952: 170026
62. Shojaei Z, Khayati G R, Darezereshki E. Review of electrodeposition methods for the preparation of high-entropy alloys. International Journal of Minerals Metallurgy and Materials, 2022, 29(9): 1683–1696
63. Erb U. Electrodeposited nanocrystals: synthesis, properties, and industrial applications. Nanostructured Materials, 1995, 6(5): 533–538
64. Brenner A. Electrodeposition of Alloys—Principles and Practice. Massachusetts: Academic Press, 1963
65. Nechvoglod O, Ostovari Moghaddam A, Pratskova S, Trofimova S, Samodurova M, Trofimov E. A review on high-entropy alloys coatings fabricated by electrodeposition: the correlation between composition, properties, and processing parameters. Journal of the Minerals Metals & Materials Society, 2025, 77(3): 1005–1028
66. Shah A, Chauhan B, Rai R, Mundotiya B. Electrodeposition of High-Entropy Alloy Coating: A Brief of the Deposition Parameters. Hyderabad: IIP Series, 2024, 61–74

67. Yao C Z, Zhang P, Liu M, Li G R, Ye J Q, Liu P, Tong Y X. Electrochemical preparation and magnetic study of Bi-Fe-Co-Ni-Mn high entropy alloy. Electrochimica Acta, 2008, 53(28): 8359–8365
68. Ujah C O, Kallon D V, Aigbodion V S. Corrosion characteristics of high-entropy alloys prepared by spark plasma sintering. International Journal of Advanced Manufacturing Technology, 2024, 132(1): 63–82
69. Ipadeola A K, Lebechi A K, Gaolatlhe L, Haruna A B, Chitt M, Eid K, Abdullah A M, Ozoemena K I. Porous high-entropy alloys as efficient electrocatalysts for water-splitting reactions. Electrochemistry Communications, 2022, 136: 107207
70. Kante M V, Weber M L, Ni S, van den Bosch I C G, van der Minne E, Heymann L, Falling L J, Gauquelin N, Tsvetanova M, Cunha D M, et al. A high-entropy oxide as high-activity electrocatalyst for water oxidation. ACS Nano, 2023, 17(6): 5329–5339
71. Fan L, Ji Y, Wang G, Chen J, Chen K, Liu X, Wen Z. High entropy alloy electrocatalytic electrode toward alkaline glycerol valorization coupling with acidic hydrogen production. Journal of the American Chemical Society, 2022, 144(16): 7224–7235
72. Song L, Ma C, Shi P, Zhu X, Qu K, Zhu L, Lu Q, Wang A L. Self-supported FeCoNiCuP high-entropy alloy nanosheet arrays for efficient glycerol oxidation and hydrogen evolution in seawater electrolytes. Green Chemistry, 2024, 26(21): 10921–10928
73. Song H, Wang J, Zhang Z, Shai X, Guo Y. Synergistic balancing hydrogen and hydroxyl adsorption/desorption of nickel sulfide via cation and anion dual-doping for boosting alkaline hydrogen evolution. Chemical Engineering Journal, 2021, 420: 129842
74. Liu Z, Ma H, Kang N, Jiang X, Chu M, Xie G, Liu X, Liu X. Nanoscale Raspberry-like Ni-Fe-Co-Mn-V high-entropy alloy electrocatalysts: a pathway to ultrlow overpotential hydrogen evolution. Materials Today Chemistry, 2024, 42: 102404
75. Zhang Z J, Yu N, Dong Y L, Han G, Hu H, Chai Y M, Dong B. High entropy catalysts in electrolytic water splitting: a review from properties to applications. Chemical Engineering Journal, 2024, 498: 155736
76. Wang L, Meng Q, Xiao M, Liu C, Xing W, Zhu J. Insights into the dynamic surface reconstruction of electrocatalysts in oxygen evolution reaction. Renewables, 2024, 2: 272–296
77. Liu P F, Yin H, Fu H Q, Zu M Y, Yang H G, Zhao H. Activation strategies of water-splitting electrocatalysts. Journal of Materials Chemistry A: Materials for Energy and Sustainability, 2020, 8(20): 10096–10129
78. Li W, Liu P, Liaw P K. Microstructures and properties of high-entropy alloy films and coatings: a review. Materials Research Letters, 2018, 6(4): 199–229
79. Ye Y F, Wang Q, Lu J, Liu C T, Yang Y. High-entropy alloy: challenges and prospects. Materials Today, 2016, 19(6): 349–362
80. Zhang F X, Song H Q. Effect of atomic size mismatch and chemical complexity on the local lattice distortion of BCC solid solution alloys. Materials Today Communications, 2022, 33: 104367
81. Tong Y, Velisa G, Zhao S, Guo W, Yang T, Jin K, Lu C, Bei H, Ko J Y P, Pagan D C, et al. Evolution of local lattice distortion under irradiation in medium- and high-entropy alloys. Materialia, 2018, 2: 73–81
82. Wang Y, Yang H, Zhang Z, Meng X, Cheng T, Qin G, Li S. Far-from-equilibrium electrosynthesis ramifies high-entropy alloy for alkaline hydrogen evolution. Journal of Materials Science and Technology, 2023, 166: 234–240
83. Priamushko T, Kormányos A, Cherevko S. What do we know about the electrochemical stability of high-entropy alloys? Current Opinion in Chemical Engineering, 2024, 44: 101020
84. Gu F, Zhang Q, Chen X H, Li T, Fu H C, Luo H Q, Li N B. Electronic regulation and core-shell hybrids engineering of palm-leaf-like NiFe/$Co(PO_3)_2$ bifunctional electrocatalyst for efficient overall water splitting. International Journal of Hydrogen Energy, 2022, 47(66): 28475–28485
85. López Ríos M, Socorro Perdomo P P, Voiculescu I, Geanta V, Crăciun V, Boerasu I, Mirza Rosca J C. Effects of nickel content on the microstructure, microhardness, and corrosion behavior of high-entropy $AlCoCrFeNi_x$ alloys. Scientific Reports, 2020, 10(1): 21119
86. He L, Wang N, Sun B, Zhong L, Yao M, Hu W, Komarneni S. High-entropy FeCoNiMn (oxy) hydroxide as high-performance electrocatalyst for OER and boosting clean carrier production under quasi-industrial condition. Journal of Cleaner Production, 2022, 356: 131680
87. Bian H, Wang C, Zhao S, Han G, Xie G, Qi P, Liu X, Zeng Y, Zhang D, Wang P. Preparation of highly efficient high-entropy alloy catalysts with electrodeposition and corrosion engineering for OER electrocatalysis. International Journal of Hydrogen Energy, 2024, 57: 651–659
88. Yang Z Z, Zhang C, Zeng G M, Tan X F, Wang H, Huang D L, Yang K H, Wei J J, Ma C, Nie K. Design and engineering of layered double hydroxide based catalysts for water depollution by advanced oxidation processes: a review. Journal of Materials Chemistry A: Materials for Energy and Sustainability, 2020, 8(8): 4141–4173
89. Gupta A K, Choudhari A, Rane A, Tiwari A, Sharma P, Gupta A, Sapale P, Tirumala R T A, Muthaiah R, Kumar A. Advances in nickel-containing high-entropy alloys: from fundamentals to additive manufacturing. Materials, 2024, 17(15): 3826
90. Li K, He J, Guan X, Tong Y, Ye Y, Chen L, Chen P. Phosphorus-modified amorphous high-entropy cofenicrmn compound as high-performance electrocatalyst for hydrazine-assisted water electrolysis. Small, 2023, 19(42): 2302130
91. Han M, Wang C, Zhong J, Han J, Wang N, Seifitokaldani A, Yu Y, Liu Y, Sun X, Vomiero A, et al. Promoted self-construction of β-NiOOH in amorphous high entropy electrocatalysts for the oxygen evolution reaction. Applied Catalysis B: Environmental, 2022, 301: 120764
92. Huang Q. Electrodeposition of FeCoNiCu quaternary system. Dissertation for the Doctoral Degree. Baton Rouge: Louisiana State University and Agricultural & Mechanical College, 2004
93. Reddy K S K J, Chokkakula L P, Dey S R. Strategies to engineer FeCoNiCuZn high entropy alloy composition through aqueous electrochemical deposition. Electrochimica Acta, 2023,

453: 142350

94. Chang S Q, Cheng C C, Cheng P Y, Huang C L, Lu S Y. Pulse electrodeposited FeCoNiMnW high entropy alloys as efficient and stable bifunctional electrocatalysts for acidic water splitting. Chemical Engineering Journal, 2022, 446: 137452
95. Huang C L, Lin Y G, Chiang C L, Peng C K, Raja D S, Hsieh C T, Chen Y A, Chang S Q, Yeh Y X, Lu S Y. Atomic scale synergistic interactions lead to breakthrough catalysts for electrocatalytic water splitting. Applied Catalysis B: Environmental, 2023, 320: 122016
96. Schweckandt D S, del Carmen Aguirre M. Electrodeposition of Ni-Co alloys determination of properties to be used as coins. Procedia Materials Science, 2015, 8: 91–100
97. Oliveira J A M, de Almeida A F, Campos A R N, Prasad S, Alves J J N, de Santana R A C. Effect of current density, temperature, and bath pH on properties of Ni-W-Co alloys obtained by electrodeposition. Journal of Alloys and Compounds, 2021, 853: 157104
98. Nourmohammadi Khiarak B, Shariati K, Mojaddami M, Zamani Z, Zekiy A O, Simchi A. Efficient electrocatalytic overall water splitting on a Cu-based high entropy alloy: an electrochemical study. Energy & Fuels, 2022, 36(8): 4502–4509
99. Yu C, Wang X W, He W X, Zheng Z Y, Dang X J, Zhang Y F. Electrodeposition of FeCoNiCuMn high-entropy alloy nanoparticles as efficient bifunctional electrolytic water catalyst. Surfaces and Interfaces, 2024, 46: 104084
100. Guo F, Yu J, Xiao J, Luoluo Q, Yang H, Guo Y. Preparation of FeCoNiCr high entropy alloy coatings and optimization of process parameters. Rare Metal Materials and Engineering, 2021, 50(7): 2337–2342
101. Li Y, Liu Y, Shen J, Lan A, Jin X, Han L, Qiao J. High-entropy amorphous FeCoCrNi thin films with excellent electrocatalytic oxygen evolution reaction performance. Journal of Alloys and Compounds, 2024, 1005: 176089
102. Aliyu A, Rekha M, Srivastava C. High Entropy Alloys. Florida: CRC Press, 2020, 313–328
103. Aliyu A, Srivastava C. Phase constitution, surface chemistry, and corrosion behavior of electrodeposited MnFeCoNiCu high entropy alloy-graphene oxide composite coatings. Surface and Coatings Technology, 2022, 429: 127943
104. Mohan M, Pandel U, Kumar K. Phase composition, surface chemistry, and electrochemical studies of electrodeposited AlMnFeCuNi high entropy alloy composite coatings incorporated with carbon nanotubes. Materials Research Express, 2024, 11(4): 046403
105. Fernández-Barcia M, Hoffmann V, Oswald S, Giebeler L, Wolff U, Uhlemann M, Gebert A. Electrodeposition of manganese layers from sustainable sulfate based electrolytes. Surface and Coatings Technology, 2018, 334: 261–268
106. Gan Y, Cui M, Dai X, Ye Y, Nie F, Ren Z, Yin X, Wu B, Cao Y, Cai R, et al. Mn-doping induced electronic modulation and rich oxygen vacancies on vertically grown $NiFe_2O_4$ nanosheet array for synergistically triggering oxygen evolution reaction. Nano Research, 2022, 15(5): 3940–3945
107. Asghari Alamdari A, Jahangiri H, Yagci M B, Igarashi K, Matsumoto H, Motallebzadeh A, Unal U. Exploring the role of Mo and Mn in improving the OER and HER performance of CoCuFeNi-based high-entropy alloys. ACS Applied Energy Materials, 2024, 7(6): 2423–2435
108. Dąbrowa J, Zajusz M, Kucza W, Cieślak G, Berent K, Czeppe T, Kulik T, Danielewski M. Demystifying the sluggish diffusion effect in high entropy alloys. Journal of Alloys and Compounds, 2019, 783: 193–207
109. Ahmadkhaniha D, Kruemmling J, Zanella C. Electrodeposition of high entropy alloy of Ni-Co-Cu-Mo-W from an aqueous bath. Journal of the Electrochemical Society, 2022, 169(8): 082515
110. Sun S, Bairachna T, Podlaha E J. Induced codeposition behavior of electrodeposited NiMoW alloys. Journal of the Electrochemical Society, 2013, 160(10): D434–D440
111. Donten M, Cesiulis H, Stojek Z. Electrodeposition and properties of Ni W, Fe W, and Fe Ni W amorphous alloys: a comparative study. Electrochimica Acta, 2000, 45(20): 3389–3396
112. Zhang B, Wang L, Cao Z, Kozlov S M, García de Arquer F P, Dinh C T, Li J, Wang Z, Zheng X, Zhang L, et al. High-valence metals improve oxygen evolution reaction performance by modulating 3d metal oxidation cycle energetics. Nature Catalysis, 2020, 3(12): 985–992
113. Bian H, Wang R, Zhang K, Zheng H, Wen M, Li Z, Li Z, Wang G, Xie G, Liu X, et al. Facile electrodeposition synthesis and super performance of nano-porous Ni-Fe-Cu-Co-W high entropy alloy electrocatalyst. Surface and Coatings Technology, 2023, 459: 129407
114. Mei Y, Feng Y, Zhang C, Zhang Y, Qi Q, Hu J. High-entropy alloy with Mo-coordination as efficient electrocatalyst for oxygen evolution reaction. ACS Catalysis, 2022, 12(17): 10808–10817
115. Cheng Z, Han X, Han L, Zhang J, Liu J, Wu Z, Zhong C. Novel high-entropy FeCoNiMoZn-layered hydroxide as an efficient electrocatalyst for the oxygen evolution reaction. Nanomaterials, 2024, 14(10): 889
116. Wang L, Gao Z, Su K, Nguyen N T, Gao R T, Chen J, Wang L. Stacked high-entropy hydroxides promote charge transfer kinetics for photoelectrochemical water splitting. Advanced Functional Materials, 2024, 34(40): 2403948
117. Hegde A C, Venkatakrishna K, Eliaz N. Electrodeposition of Zn-Ni, Zn-Fe, and Zn-Ni-Fe alloys. Surface and Coatings Technology, 2010, 205(7): 2031–2041
118. Okonkwo B O, Jeong C, Lee H B, Jang C, Rahimi E, Davoodi A. Development and optimization of trivalent chromium electrodeposit on 304L stainless steel to improve corrosion resistance in chloride-containing environment. Heliyon, 2023, 9(12): e22538
119. Shi Y, Zhang B. Recent advances in transition metal phosphide nanomaterials: synthesis and applications in hydrogen evolution reaction. Chemical Society Reviews, 2016, 45(6): 1529–1541
120. Li S, Wang L, Su H, Hong A N, Wang Y, Yang H, Ge L, Song W, Liu J, Ma T, et al. Electron redistributed S-doped nickel iron phosphides derived from one-step phosphatization of MOFs for significantly boosting electrochemical water splitting. Advanced Functional Materials, 2022, 32(23): 2200733
121. Bachvarov V, Arnaudova M, Rashkov R S, Zielonka A.

Electrochemical deposition of alloys based on Ni-Fe-Co, containing W, P, and their characterization for hydrogen evolution reaction. Izvestiia po Himiia, 2011, 43(1): 115–119

122. Yang D, Hou W, Lu Y, Zhang W, Chen Y. Cobalt phosphide nanoparticles supported within network of N-doped carbon nanotubes as a multifunctional and scalable electrocatalyst for water splitting. Journal of Energy Chemistry, 2021, 52: 130–138
123. Chen Q, Han X, Xu Z, Chen Q, Wu Q, Zheng T, Wang P, Wang Z, Wang J, Li H, et al. Atomic phosphorus induces tunable lattice strain in high entropy alloys and boosts alkaline water splitting. Nano Energy, 2023, 110: 108380
124. Białostocka A M, Klekotka U, Kalska-Szostko B. The effect of a substrate material on composition gradients of Fe-Ni films obtained by electrodeposition. Scientific Reports, 2020, 10(1): 1029
125. Popescu A M J, Branzoi F, Burada M, Moreno J C, Anastasescu M, Anasiei I, Olaru M T, Constantin V. CoCrFeMnNi high-entropy alloy thin films electrodeposited on aluminum support. Coatings, 2023, 13(6): 980
126. Sun H, Kim H, Song S, Jung W. Copper foam-derived electrodes as efficient electrocatalysts for conventional and hybrid water electrolysis. Materials Reports: Energy, 2022, 2(2): 100092
127. Yu G, Xie X, Pan L, Bao Z, Cui Y. Hybrid nanostructured materials for high-performance electrochemical capacitors. Nano Energy, 2013, 2(2): 213–234
128. Xu Z, Wang Y, Gao X, Peng L, Qiao Q, Xiao J, Guo F, Wang R, Yu J. Electrochemical deposition and corrosion resistance characterization of FeCoNiCr high-entropy alloy coatings. Coatings, 2023, 13(7): 1167
129. Ju L, Wu W, Zhou Y, Zhang Y, Wang Q. Electrodeposition of FeNiCoCrMn high-entropy alloys on copper foam for enhanced hydrogen evolution reaction—influence of additives and deposition potential. Materials Letters, 2024, 374: 137195
130. Zheng W, Liu M, Lee L Y S. Best practices in using foam-type electrodes for electrocatalytic performance benchmark. ACS Energy Letters, 2020, 5(10): 3260–3264
131. Jin Y, Zhang T, Pan N, Wang S, Zhang B, Zhu X, Hao Y, Wang X, Song L, Zhang M. Surface functionalization of carbon cloth with conductive Ni/Fe-MOFs for highly efficient oxygen evolution. Surfaces and Interfaces, 2022, 33: 102294
132. Zhang T, Li J, Zhang B, Wang G, Jiang K, Zheng Z, Shen J. High-entropy alloy CuCrFeNiCoP film of Cu-based as high-efficiency electrocatalyst for water splitting. Journal of Alloys and Compounds, 2023, 969: 172439
133. Haché M J R. Synthesis and characterization of electrodeposited nanocrystalline medium- and high-entropy alloys. Dissertation for the Doctoral Degree. Toronto: University of Toronto, 2023
134. Soare V, Burada M, Constantin I, Mitrică D, Bădiliţă V, Caragea A, Târcolea M. Electrochemical deposition and microstructural characterization of AlCrFeMnNi and AlCrCuFeMnNi high entropy alloy thin films. Applied Surface Science, 2015, 358: 533–539
135. Popescu A M J, Branzoi F, Constantin I, Anastasescu M, Burada M, Mitrică D, Anasiei I, Olaru M T, Constantin V. Electrodeposition, characterization, and corrosion behavior of CoCrFeMnNi high-entropy alloy thin films. Coatings, 2021, 11(11): 1367
136. Wen B, Zhao X, Dong Q, Li B, Lyu X. Gradient composition design of FeCoCrMnNi high entropy alloys: an efficient and stable electrocatalyst for water splitting. Journal of Power Sources, 2025, 627: 235804
137. Obradović M, Stevanović R M, Despić A R. Electrochemical deposition of Ni-W alloys from ammonia-citrate electrolyte. Journal of Electroanalytical Chemistry, 2003, 552: 185–196
138. El-Sherik A M, Er U. Synthesis of bulk nanocrystalline nickel by pulsed electrodeposition. Journal of Materials Science, 1995, 30(22): 5743–5749
139. Glasscott M W, Pendergast A D, Goines S, Bishop A R, Hoang A T, Renault C, Dick J E. Electrosynthesis of high-entropy metallic glass nanoparticles for designer, multi-functional electrocatalysis. Nature Communications, 2019, 10(1): 2650
140. Murakami Y, Murase K, Fukami K. Smooth thin film of a CoNiCu medium-entropy alloy consisting of single nanometer-sized grains formed by electrodeposition in a water-in-oil emulsion. Journal of Physical Chemistry C, 2023, 127(9): 4696–4703
141. Glasscott M W, Pendergast A D, Dick J E. A universal platform for the electrodeposition of ligand-free metal nanoparticles from a water-in-oil emulsion system. ACS Applied Nano Materials, 2018, 1(10): 5702–5711
142. Wasekar N P, Hebalkar N, Jyothirmayi A, Lavakumar B, Ramakrishna M, Sundararajan G. Influence of pulse parameters on the mechanical properties and electrochemical corrosion behavior of electrodeposited Ni-W alloy coatings with high tungsten content. Corrosion Science, 2020, 165: 108409
143. Ahmadkhaniha D, Ascani D, Fedel M, Zanella C. Electrodeposition and properties of Ni-Co-W-(Mo-Cu) high/medium entropy alloy coatings deposited from an aqueous bath. Intermetallics, 2025, 181: 108744
144. Xiao T, Sun C, Wang R. Electrodeposited CrMnFeCoNi Oxy-carbide film and effect of selective dissolution of Cr on oxygen evolution reaction. Journal of Materials Science and Technology, 2024, 200: 176–184
145. Santana R A C, Campos A R N, Medeiros E A, Oliveira A L M, Silva L M F, Prasad S. Studies on electrodeposition and corrosion behaviour of a Ni-W-Co amorphous alloy. Journal of Materials Science, 2007, 42(22): 9137–9144
146. Farzaneh M, Raeissi K, Golozar M. Effect of current density on deposition process and properties of nanocrystalline Ni-Co-W alloy coatings. Journal of Alloys and Compounds, 2010, 489(2): 488–492
147. Tsyntsaru N, Cesiulis H, Donten M, Sort J, Pellicer E, Podlaha-Murphy E J. Modern trends in tungsten alloys electrodeposition with iron group metals. Surface Engineering and Applied Electrochemistry, 2012, 48(6): 491–520
148. Giovanardi R, Orlando G. Chromium electrodeposition from Cr(III) aqueous solutions. Surface and Coatings Technology, 2011, 205(15): 3947–3955
149. Zhang W, Xia W, Li B, Li M, Hong M, Zhang Z. Influences of Co and process parameters on structure and corrosion properties of nanocrystalline Ni-W-Co ternary alloy film fabricated by

electrodeposition at low current density. Surface and Coatings Technology, 2022, 439: 128457

150. Zhang H M, Zuo L, Gao Y, Guo J, Zhu C, Xu J, Sun J. Amorphous high-entropy phosphoxides for efficient overall alkaline water/seawater splitting. Journal of Materials Science and Technology, 2024, 173: 1–10
151. Mo D, Zhang J, Chen G, Huang Z, Liu X, Cai W, Cui J, Su W. Stirred-electrodeposition construction of porous Fe-doped NiSe nanoclusters as a bifunctional catalyst for water splitting. Journal of Alloys and Compounds, 2024, 1002: 175090
152. Chou H L, Hwang B J, Sun C L. New and Future Developments in Catalysis. Amsterdam: Elsevier, 2013, 217–270
153. Denuault G, Sosna M, Williams K J. Handbook of Electrochemistry. Amsterdam: Elsevier, 2007, 431–469
154. Hadipour A, Bharololoom M E. Influence of type of bath agitation (magnetic stirring and rotating disk cathode) on tribological properties of nickel electrodeposits. Protection of Metals and Physical Chemistry of Surfaces, 2018, 54(2): 274–281
155. Syamsuir S, Susetyo F B, Anggrainy R, Lubi A, Soegijono B, Rosyidan C, Yudanto S D, Situmorang E U M, Nanto D. Electrolyte solution stirring effect on deposition rate, crystallographic orientation, and electrochemical behaviour of Ni film. Journal of Physics: Conference Series, 2024, 2866(1): 012001
156. Mamaghani K R, Naghib S M. The effect of stirring rate on electrodeposition of nanocrystalline nickel coatings and their corrosion behaviors and mechanical characteristics. International Journal of Electrochemical Science, 2017, 12(6): 5023–5035
157. Srimathi S, Mayanna S, Sheshadri B. Electrodeposition of binary magnetic alloys. Surface Technology, 1982, 16(4): 277–322
158. Farias L T D, Luna A S, Lago D C B D, Senna L F D. Influence of cathodic current density and mechanical stirring on the electrodeposition of Cu-Co alloys in citrate bath. Materials Research, 2008, 11(1): 1–9
159. Aliyu A, Rekha M, Srivastava C. Microstructure-electrochemical property correlation in electrodeposited CuFeNiCoCr high-entropy alloy-graphene oxide composite coatings. Philosophical Magazine, 2019, 99(6): 718–735
160. Liu Z, Liu Z, Zan L, Sun Y, Han H, Li Z, Wan H, Cao T, Zhu Y, Lv H. *In situ* anodic transition and cathodic contamination affect the overall voltage of alkaline water electrolysis. Molecules, 2024, 29(22): 5298
161. Freitas G, Gomes W S, Souza J P I, Pinotti C, Passamani E, Montemor M, Della Noce R. Direct electrodeposition of CoFeNiMoW high entropy alloy thin films from aqueous medium. Materials Chemistry and Physics, 2023, 309: 128438
162. Ashraf M A, Li C, Pham B T, Zhang D. Electrodeposition of Ni-Fe-Mn ternary nanosheets as affordable and efficient electrocatalyst for both hydrogen and oxygen evolution reactions. International Journal of Hydrogen Energy, 2020, 45(46): 24670–24683
163. Baek J, Hossain M D, Mukherjee P, Lee J, Winther K T, Leem J, Jiang Y, Chueh W C, Bajdich M, Zheng X. Synergistic effects of mixing and strain in high entropy spinel oxides for oxygen evolution reaction. Nature Communications, 2023, 14(1): 5936
164. Asim M, Hussain A, Kanwal S, Ahmad A, Aykut Y, Bayrakçeken A, Janjua N K. Rapid microwave synthesis of medium and high entropy oxides for outstanding oxygen evolution reaction performance. Materials Advances, 2024, 5(21): 8490–8504
165. Mohanty B, Pradhan L, Satpati B, Rajput P, Ghorbani-Asl M, Wei Y, Menezes P W, Krasheninnikov A V, Jena B K. Structural and compositional optimization of bimetallic NiCo alloy nanoparticles for promotion of alkaline hydrogen evolution reaction. Journal of Power Sources, 2025, 625: 235641
166. Bao F, Kemppainen E, Dorbandt I, Bors R, Xi F, Schlatmann R, Van de Krol R, Calnan S. Understanding the hydrogen evolution reaction kinetics of electrodeposited nickel-molybdenum in acidic, near-neutral, and alkaline conditions. ChemElectroChem, 2021, 8(1): 195–208
167. Ghadge S D, Velikokhatnyi O I, Datta M K, Shanthi P M, Tan S, Damodaran K, Kumta P N. Experimental and theoretical validation of high efficiency and robust electrocatalytic response of one-dimensional (1D) (Mn, Ir)O_2:10F nanorods for the oxygen evolution reaction in PEM-based water electrolysis. ACS Catalysis, 2019, 9(3): 2134–2157
168. Fan Z, Mucalo M, Kennedy J, Yang F. The potential of high-entropy alloys as catalyst materials in water-splitting application. International Journal of Hydrogen Energy, 2025, 134: 64–83
169. Gong S, Meng Y, Jin Z, Hsu H Y, Du M, Liu F. Recent progress on the stability of electrocatalysts under high current densities toward industrial water splitting. ACS Catalysis, 2024, 14(19): 14399–14435